BERKELEY LAB

Ion Beam Analysis in Materials Science (Rutherford backscattering and related techniques)

Kin Man Yu

Electronic Materials Program, Materials Sciences Division,
Lawrence Berkeley National Laboratory, Berkeley, CA 94720

(510) 486-6656
Kmyu@lbl.gov

Outline

- Introduction:
  - General aspects of ion beam analysis
  - Equipment
- Rutherford backscattering spectrometry (RBS)
  - Introduction-history
  - Basic concepts of RBS
    - Kinematic factor (K)
    - Scattering cross-section
    - Depth scale
  - Quantitative thin film analysis
  - Pitfalls
- Particle induced x-ray emission (PIXE)
- Hydrogen Forward Scattering
- Non-Rutherford scattering and nuclear reaction analysis
- Ion channeling
  - Minimum yield and critical angle
  - Dechanneling by defects
  - Impurity location

References

- **Books:**
  - *Backscattering Spectrometry*, Wei-Kan Chu, James W. Mayer and Marc-A. Nicolet, (Academic Press, New York 1978).
  - *Handbook of modern ion beam materials analysis,* edited by J.R. Tesmer and M. Nastasi (MRS, pittsburgh, 1995).
  - *Materials Analysis by Ion Channeling*, L. C. Feldman, J. W. Mayer and S. T. Picraux, (Academic Press, New York 1982).
  - Ion Beam Materials Analysis, edited by J. R. Bird and J. S. Williams, (Academic Press, Australia 1989).
  - *Fundamentals of Surface and Thin Film Analysis*, L. C. Feldman and J. W. Mayer (Elsevier Science, New York 1986).
  - *Encyclopedia of Materials Characterization*, edited by C. R. Brundle, C. A. Evans, Jr., S. Wilson, (Butterworth-Heinemann, Stoneham, MA 1992).
- **Review Articles:**
  - W-K. Chu, J. W. Mayer, M-A. Nicolet, G. Amsel, T. Buck, and F. H. Eisen, “Principles and applications of ion beam techniques for the analysis of solids and thin films,” Thin Solid Films **17**, 1 (1973).
  - L. C. Feldman, “ MeV ion scattering for surface structure determination,” C. R. C. Crit. Rev. Solid State and Mater. Sci. **10**, 143 (1981).
  - D. David, “New trends in ion-beam analysis,” Surf. Sci. Rep. **16**, 333 (1992).
  - W. K. Chu and J. R. Liu, “Rutherford backscattering spectrometry: reminiscences and progresses,” Mater. Chem. Phys. **46**, 183 (1996).

- http://www.eaglabs.com/en-US/references/tutorial/rbstheo/cairtheo.html

Ion Beam Analysis: General

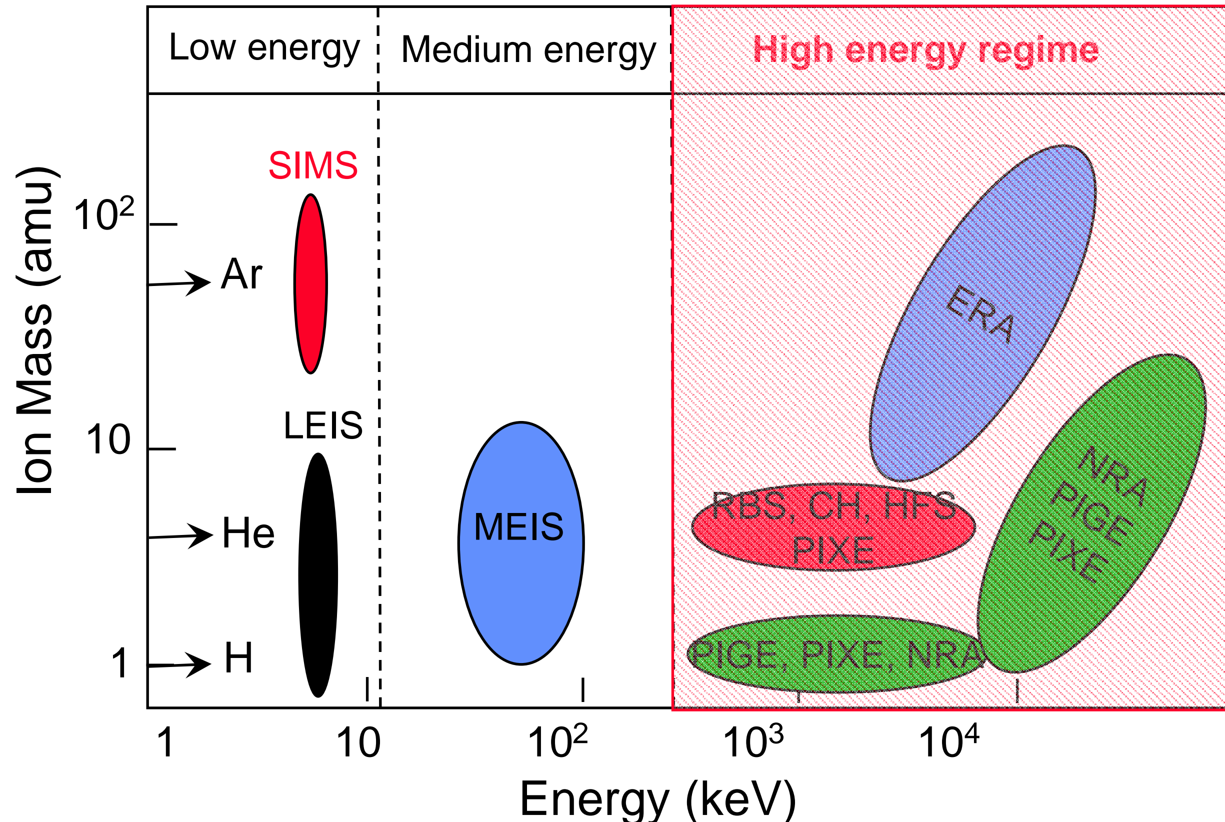

CH	-Channeling	PIGME	-Particle Induced Gamma-ray Emission
ERA	-Elastic Recoil Analysis	SIMS	-Secondary Ion Mass Spectrometry
RBS	-Rutherford Backscattering	MEIS	-Medium Energy Ion Scattering
NRA	-Nuclear Reaction Analysis	LEIS	-low energy ion scattering
PIXE	-Particle Induced X-ray Emission	HFS	-hydrogen forward scattering

MeV Ion Beam Techniques

Particle induced x-ray emission (PIXE)

$h\nu$

Rutherford backscattering spectrometry (RBS)

MeV H^+, $^4He^+$

m, E_o

$E_1 = k(m, M, \theta) E_0$

Particle induced γ-ray emission (PIGE)

m, E_1

θ

$M_1 > M_2 > m > M_3$

M_1

M_2

M_3

Elastic recoil detection (ERA)

Hydrogen forward scattering (HFS)

Ion Beam techniques

Technique	Typical Applications	Elements detected	Depth probed	Depth resolution	lateral resolution	Detection limit	Quanti-tative	Depth profiling
RBS	•thin film composition and thickness •impurity profiles •thin film interactions and interdiffusions	B-U	1-2μm	20-200Å	0.5-1mm	1-10 at.% Z<20 0.01-1 at.% 0.01-0.001at.% Z>70	Yes	Yes
PIXE	•element identification •impurity analysis	Al-U	up to 10μm	poor	0.5-1mm	0.001 at.%	Yes	No
HFS	•hydrogen or deuterium in thin films	H, d	1μm	500Å	2-3 mm	0.01 at.%	Yes	Yes
non-RBS	•Composition of thin oxide, nitride, carbide films	B, C, N, O, Si	up to 10μm	200Å	0.5-1 mm	0.1 at.%	Yes	Yes
NRA	•profiling of light elements in heavy matrix	H, B, C, N, O, F	up to a few μm	500-1000Å	0.5-1mm	0.001-1 at.%	Yes	Yes
Channeling	•crystalline quality of thin films •lattice location of impurity in single crystal •strains in pseudomorphic thin films •implantation damage analysis	B-U	1-2μm	20-200Å	0.5-1mm	0.0001 at.%	Yes	Yes

Experimental Setup

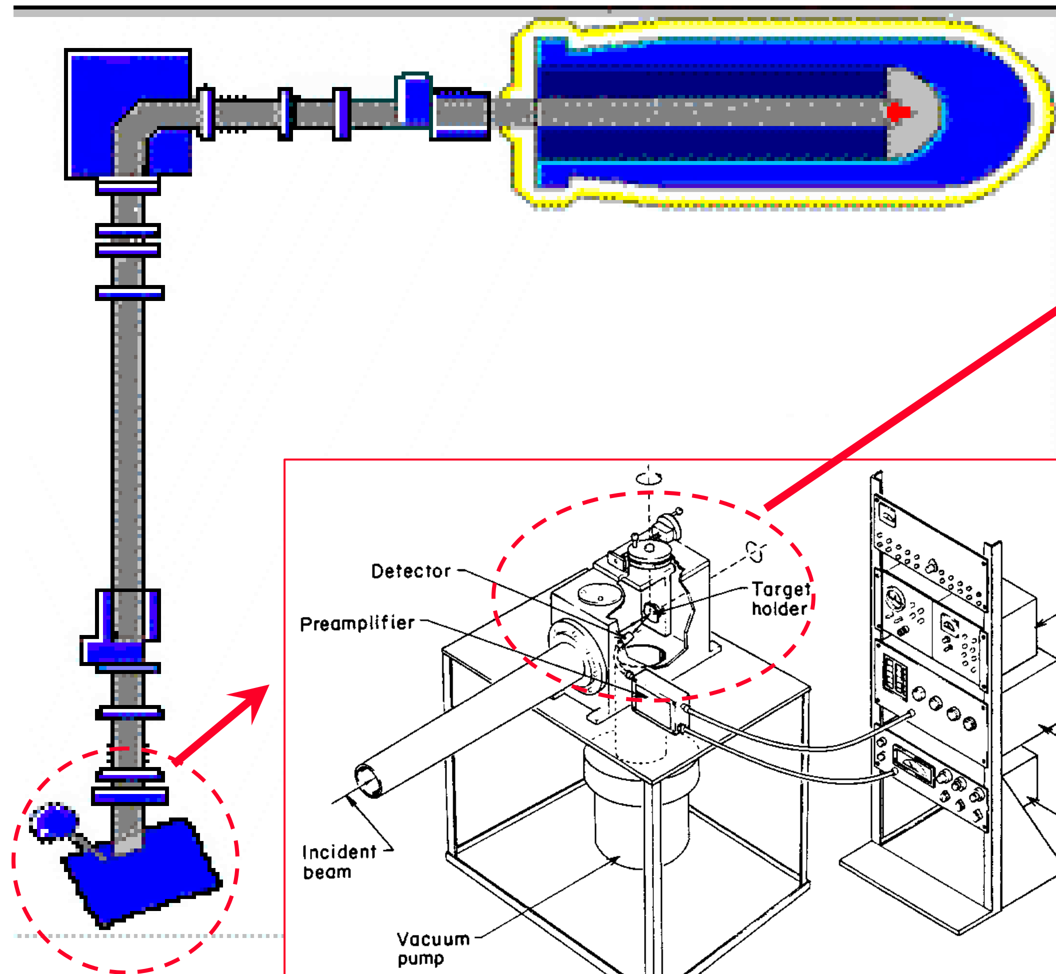

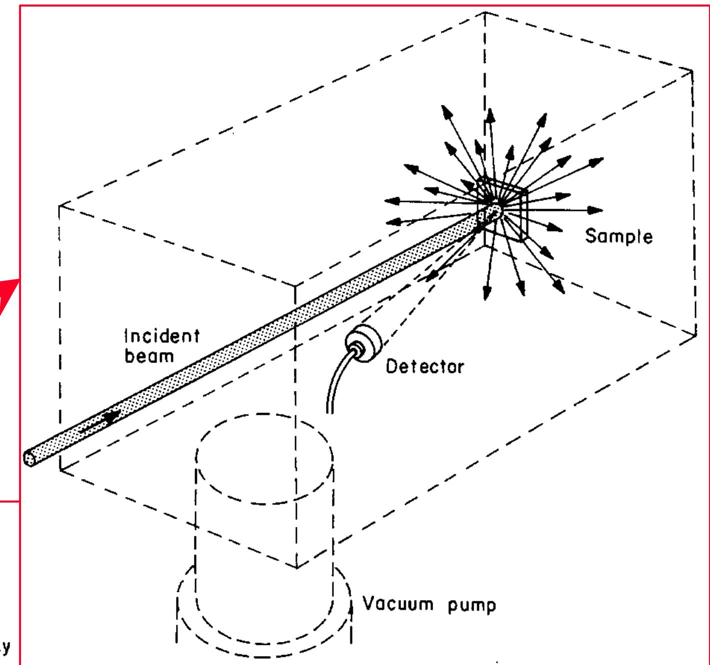

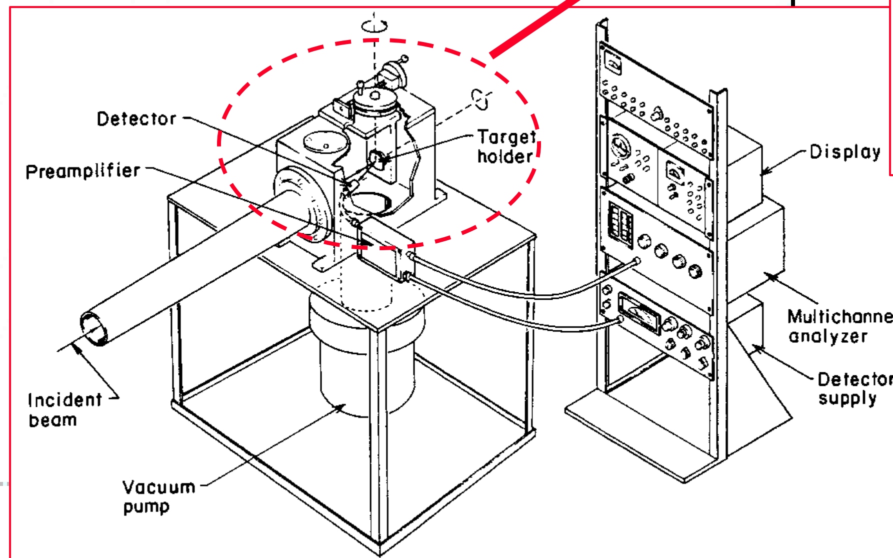

An Ideal IBA Laboratory

A compact RBS System

BERKELEY LAB

NEC MAS1000

Rutherford Backscattering Spectrometry (RBS)

Rutherford Backscattering Spectrometry (RBS)– a brief history

The original experiment

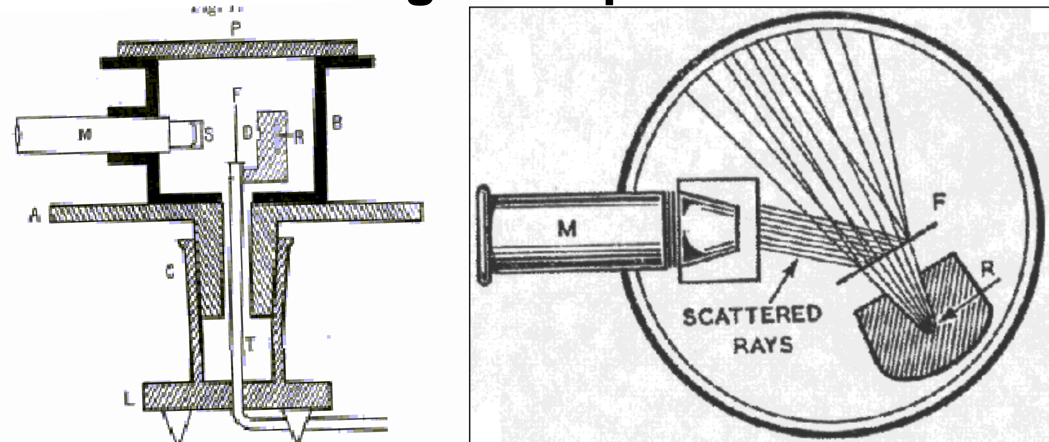

Alpha particles at a thin gold foil experiment by Hans Geiger and Ernest Marsden in 1909.

1) Almost all of the alpha particles went through the gold foil
2) Some of the alpha particles were deflected only slightly, usually 2° or less.
3) A very, very few (1 in 8000 for platinum foil) alpha particles were turned through an angle of 90° or more.

"We shall suppose that for distances less that 10^{-12} cm the central charge and also the charge on the alpha particle may be supposed to be concentrated at a point." (1911)

RBS: The Surveyor V experiment

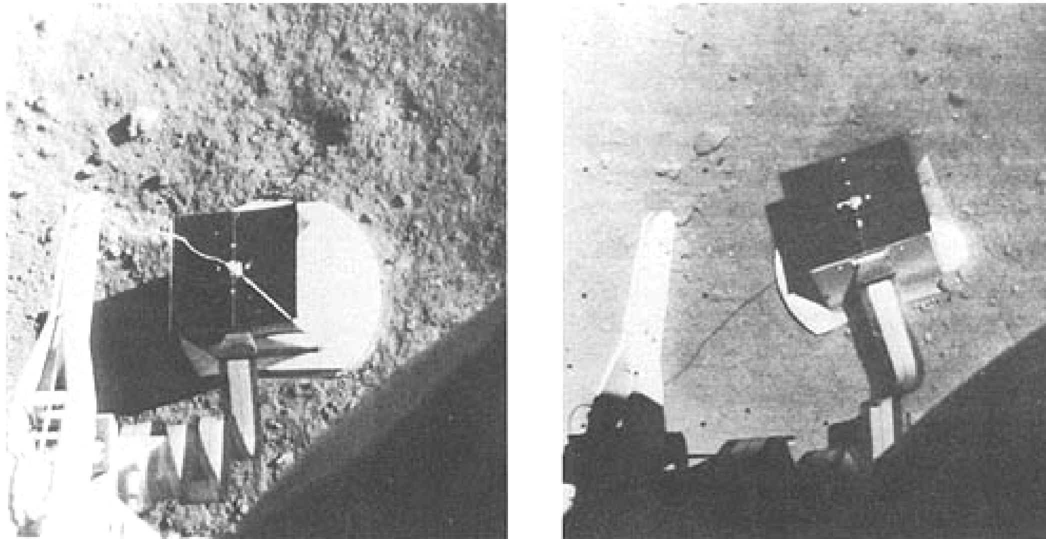

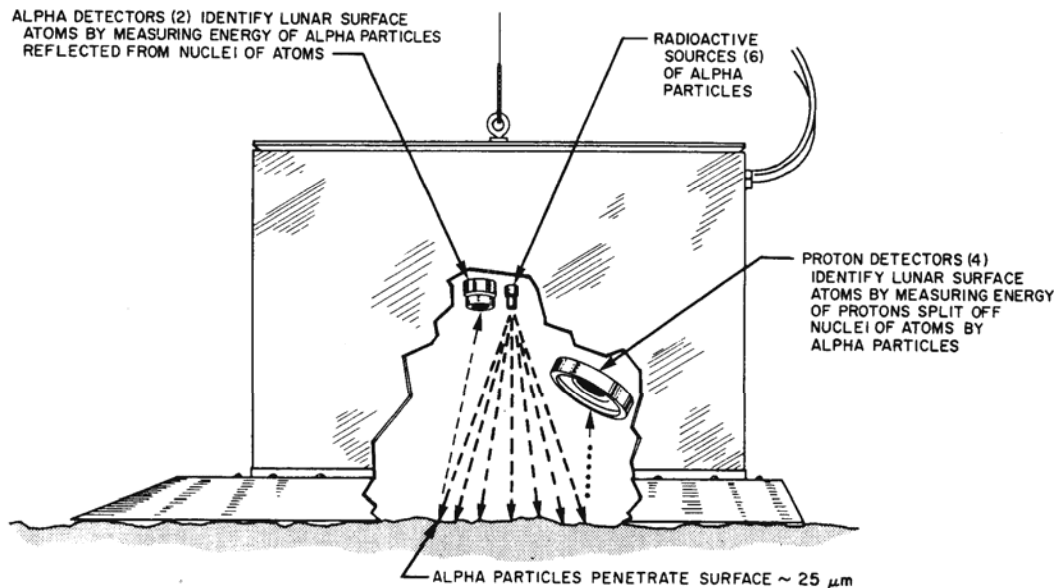

Surveyor V, first of its spacecraft family to obtain information about the chemical nature of the Moon's surface, landed in Mare Tranquillitatis on September 11, **1967**.

"**Surveyor V** carried an instrument to determine the principal chemical elements of the lunar-surface material," explained ANTHONY TURKEVICH, Enrico Fermi institute and Chemistry Department, University of Chicago. "After landing, upon command from Earth, the instrument was lowered by a nylon cord to the surface of the Moon …"

General applications of RBS

- **Quantitative analysis of thin films**
  - thickness, composition, uniformity in depth
  - Solid state reactions
  - interdiffusion
- **Crystalline perfection of homo- and heteroepitaxial thin films**
- **Quantitative measurements of impurities in substrates**
- **Defect distribution in single-crystal samples**
- **Surface atom relaxation in single crystals**
- **Lattice location of impurities in single crystals**

Strengths of RBS

- Simple in principle
- Fast and direct
- Quantitative without standard
- Depth profiling without chemical or physical sectioning
- Non-destructive
- Wide range of elemental coverage
- No special specimen preparation required
- Can be applied to crystalline or amorphous materials
- Simultaneous analysis with various ion beam techniques (PIXE, PIGE, channeling, etc.)

Radiation Damage of RBS

2 MeV $^4He^+$ in Si

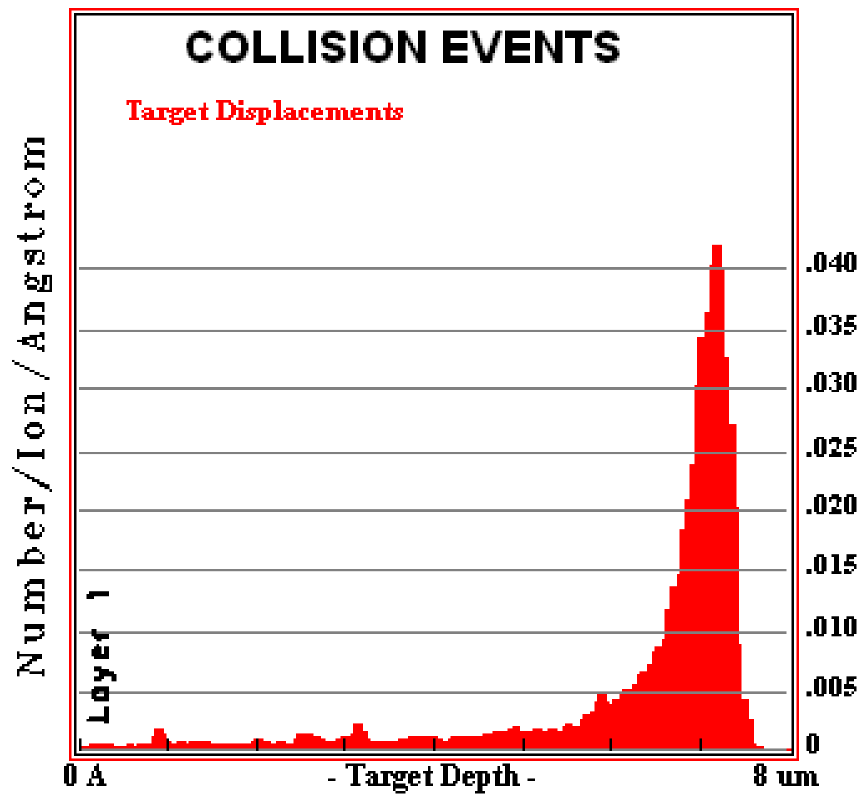

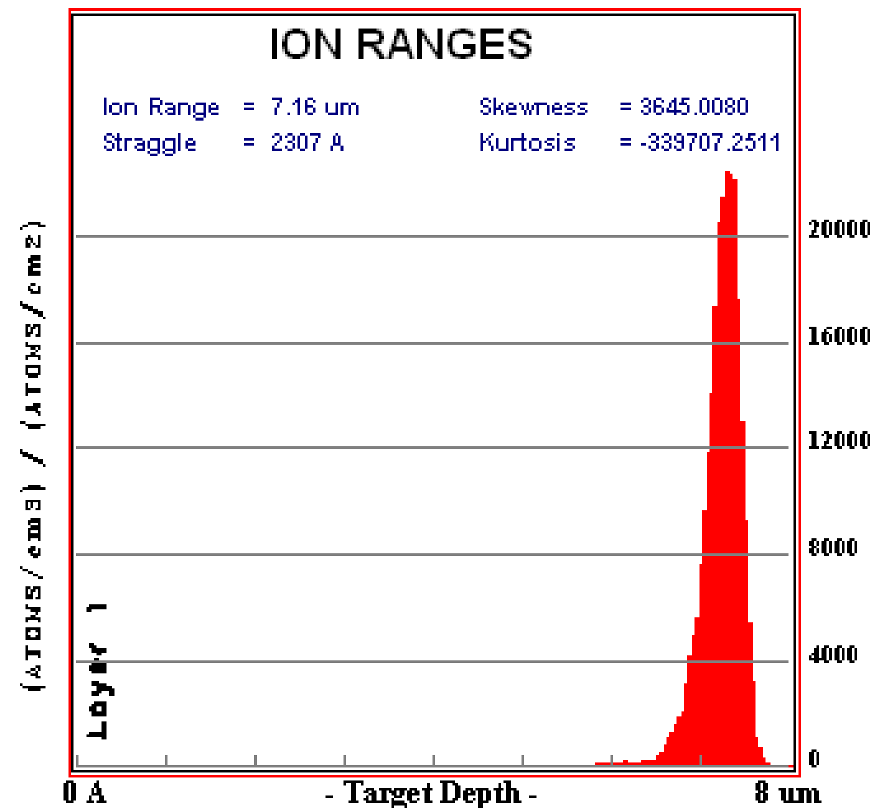

Basic concepts of RBS

- **Kinematic factor:** **elastic energy transfer from a projectile to a target atom can be calculated from collision kinematics**
  - mass determination
- **Scattering cross-section:** **the probability of the elastic collision between the projectile and target atoms can be calculated**
  - quantitative analysis of atomic composition
- **Energy Loss:** **inelastic energy loss of the projectile ions through the target**
  - perception of depth

These allow RBS analysis to give quantitative depth distribution of targets with different masses

Kinematic factor: *K*

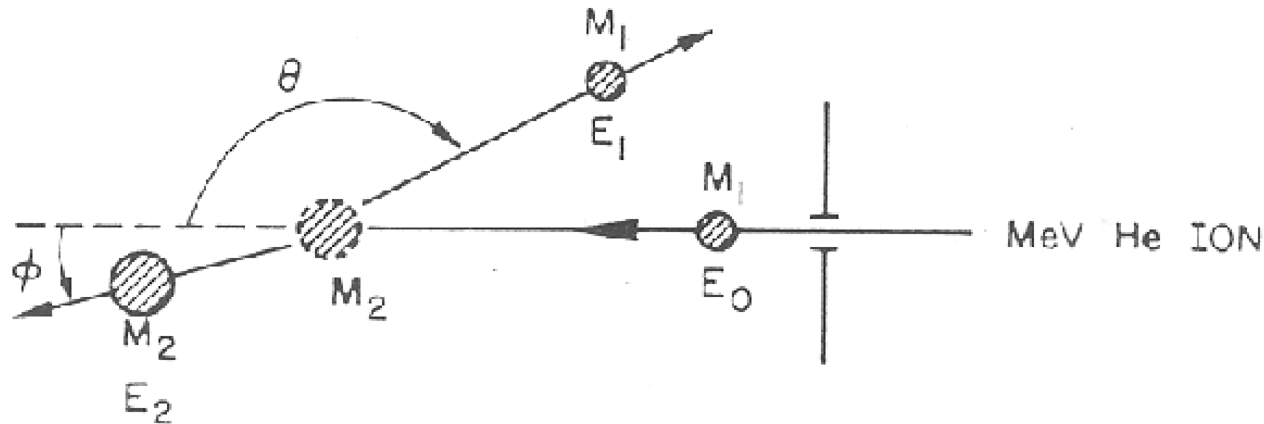

Conservation of energy :

$$\frac{1}{2}m_1v^2 = \frac{1}{2}m_1{v_1}^2 + \frac{1}{2}m_2{v_2}^2$$

Conservation of momentum:

$$m_1v = m_1v_1\cos\theta + m_2v_2\cos\phi$$

$$m_1v_1\sin\theta = m_2v_2\sin\phi$$

$$K_{m_2} = \frac{E_1}{E_o} = \left[\frac{\sqrt{(m_2^2 - m_1^2\sin^2\theta)} + m_1\cos\theta}{(m_2 + m_1)}\right]^2 = K(\theta, m_2, m_1)$$

Kinematic Factor

$$K_{m_2} = \frac{E_1}{E_o} = \left[\frac{\sqrt{(m_2^2 - m_1^2 \sin^2 \theta)} + m_1 \cos\theta}{(m_2 + m_1)} \right]^2$$

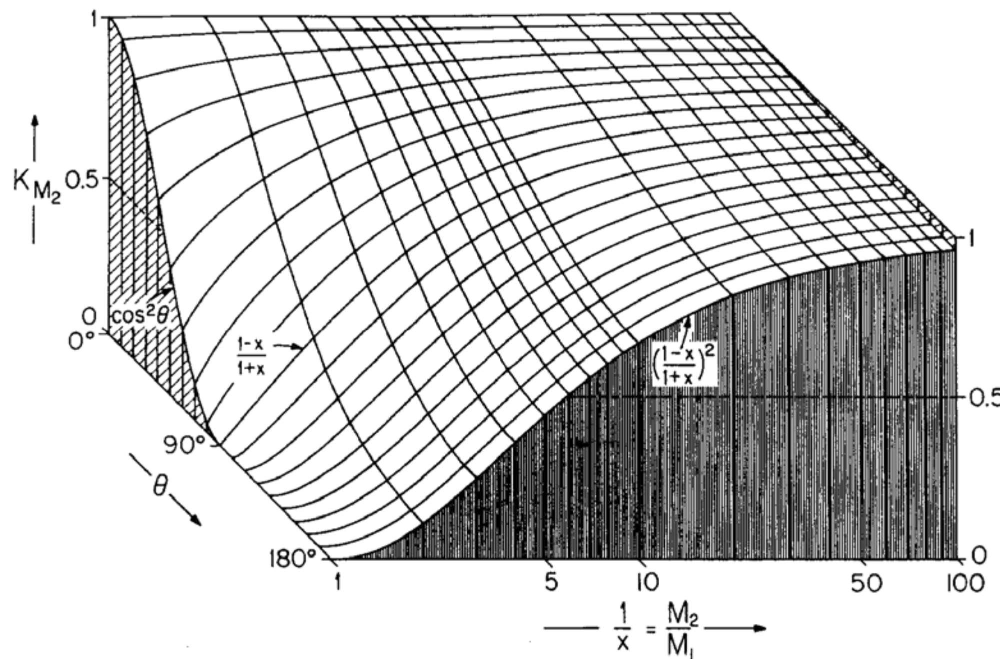

$$K_{m_2}(\theta = 180^o) = \left[\frac{(m_2 - m_1)}{(m_2 + m_1)} \right]^2$$

$$K_{m_2}(\theta = 90^o) = \frac{(m_2 - m_1)}{(m_2 + m_1)}$$

When $m_2 >> m_1$:

$$K_{m_2}(\theta = 180^o) \sim 1$$

Element identification

2.5 MeV He ion with θ=170°

K(^{197}Au) = 0.923

K(^{109}Ag) = 0.864

K(^{107}Ag) = 0.862

K(^{65}Cu) = 0.783

K(^{63}Cu) = 0.777

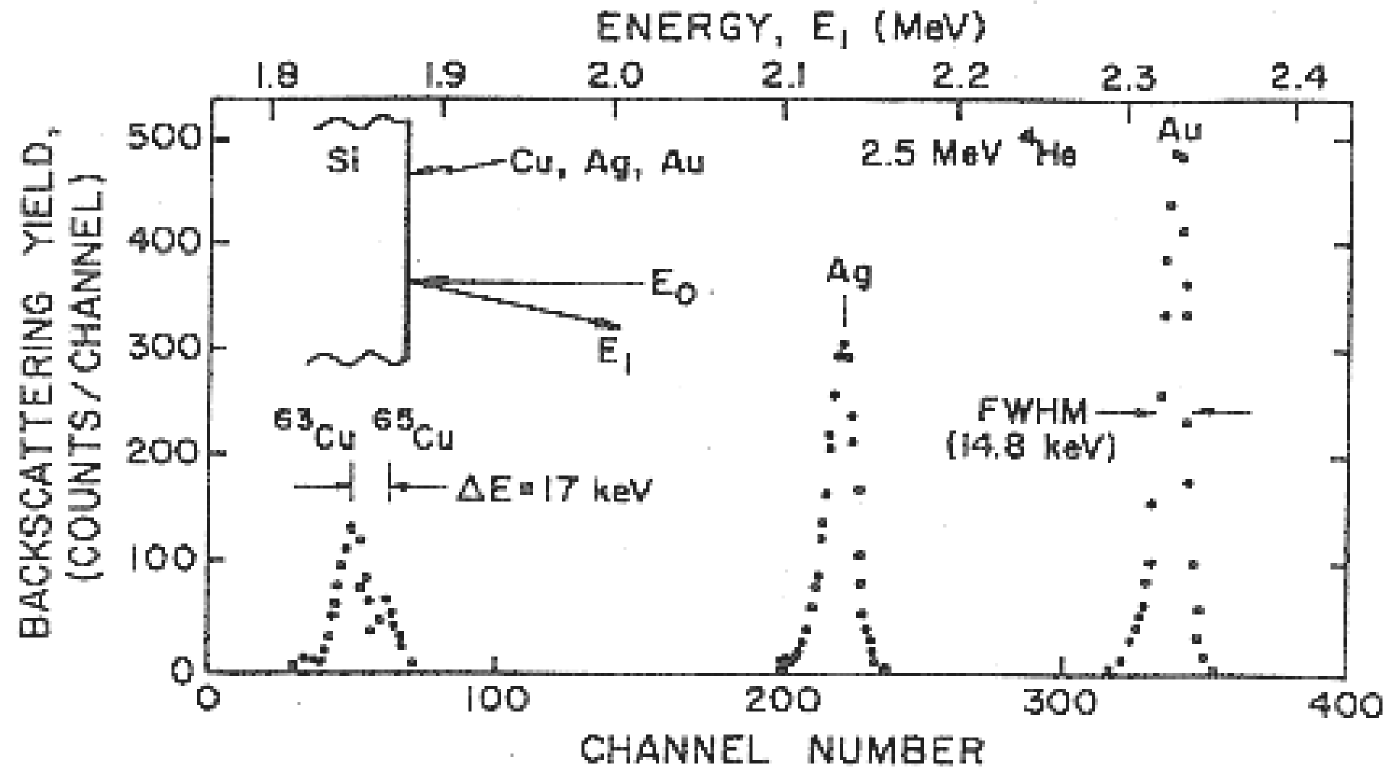

Mass Resolution, δm_2

For 180° scattering: $K_{m_2} = \frac{E_1}{E_0} = \left[\frac{(m_2 - m_1)}{(m_2 + m_1)}\right]^2$

$$\frac{\delta E_1}{E_0} = \delta \frac{(m_2 - m_1)^2}{(m_1 + m_2)^2} \qquad \therefore \delta m_2 = \frac{(m_2 + m_1)^3}{4m_1(m_2 - m_1)} \frac{\delta E_1}{E_0}$$

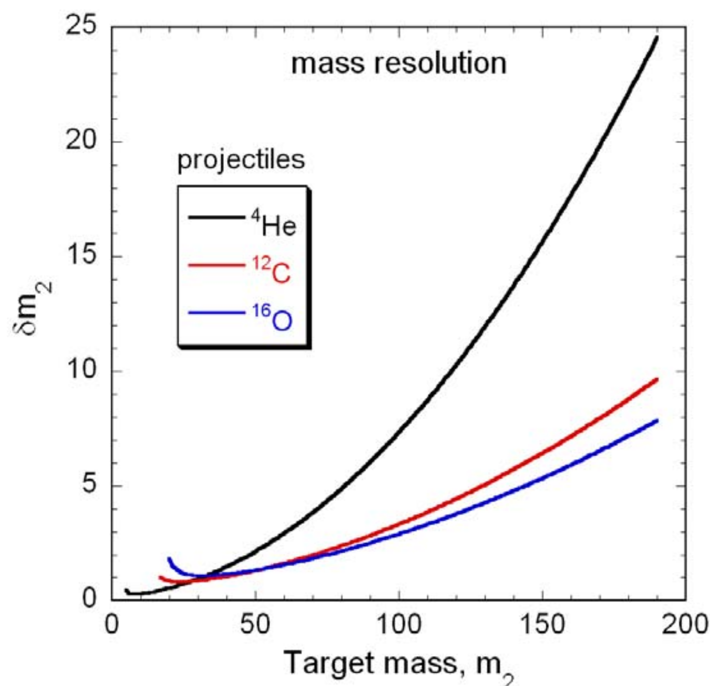

For a fixed $\delta E_1/E_0$ (~0.01), heavier projectiles result in better mass resolution

However, δE_1 for heavier projectiles is higher

Mass Resolution: Examples

With system energy resolution δE = 20keV and E_0=2MeV

For m_2=40

$$\delta m_2 = \frac{(40+4)^3}{4\times 4(40-4)} \bullet \frac{20}{2000} = 1.48 a.m.u.$$

For m_2 = 70

$$\delta m_2 = \frac{(70+4)^3}{4\times 4(70-4)} \bullet \frac{20}{2000} = 3.84 a.m.u.$$

Isotopes of Ga (68.9 and 70.9 a.m.u.) cannot be resolved

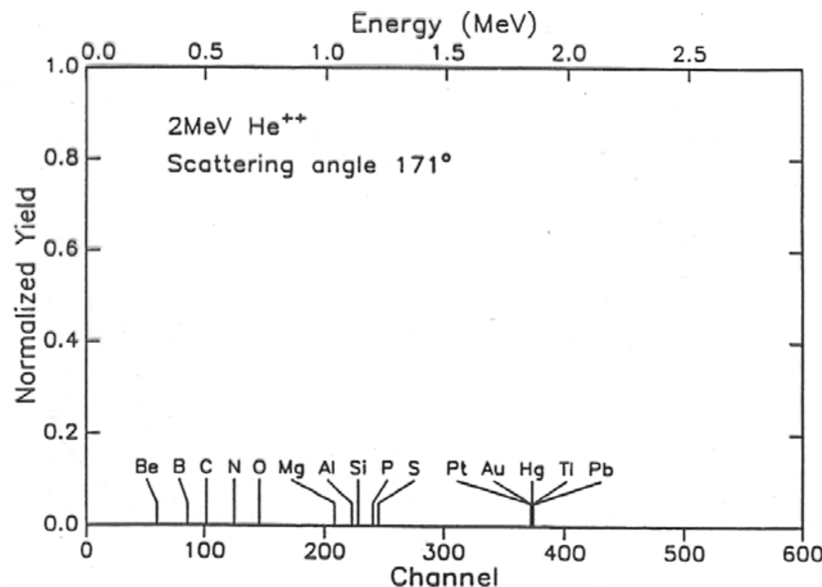

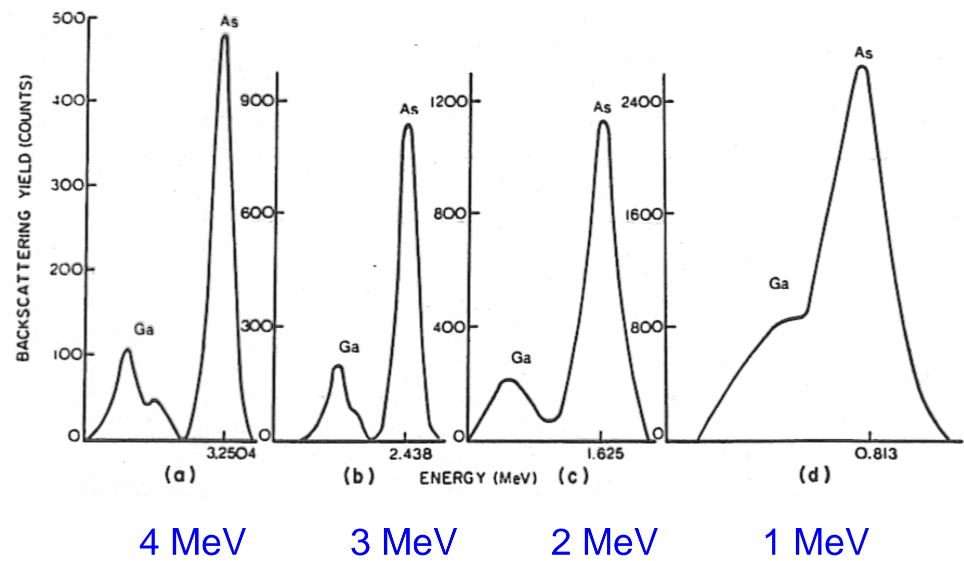

4 MeV 3 MeV 2 MeV 1 MeV

RBS Quantification

Backscattering Yield

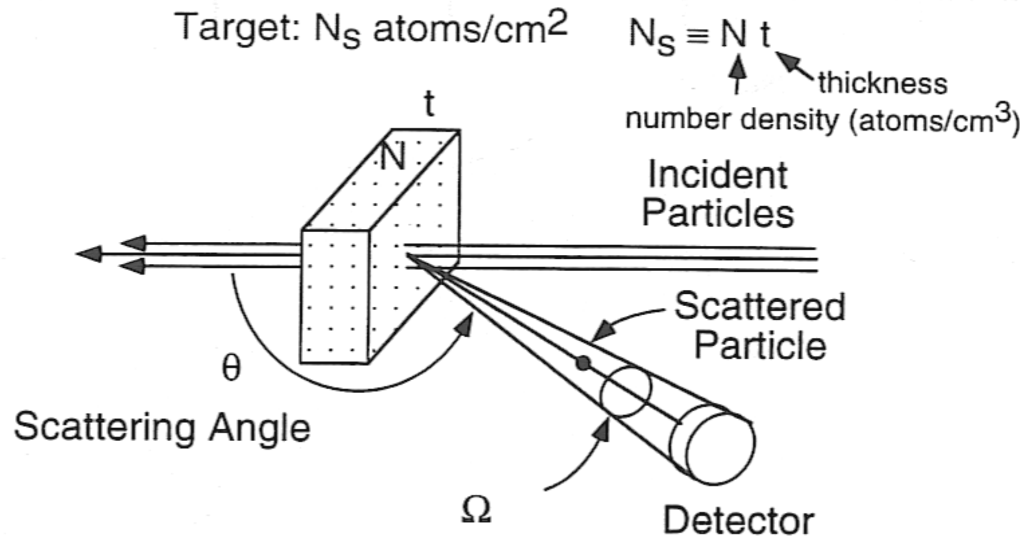

$$A = \sigma \Omega N_S Q$$

- # of particles detected
- 'average cross section'
- detector solid angle
- atoms/cm^2
- total number of incident particles

- For a given incident number of particles Q, a greater amount of an element present (N_s) should result in a greater number of particles scattered.
- Thus we need to know how often scattering events should be detected (A) at a characteristic energy ($E = KE_0$) and angle θ, within our detector's window of solid angle Ω.

Scattering cross-section

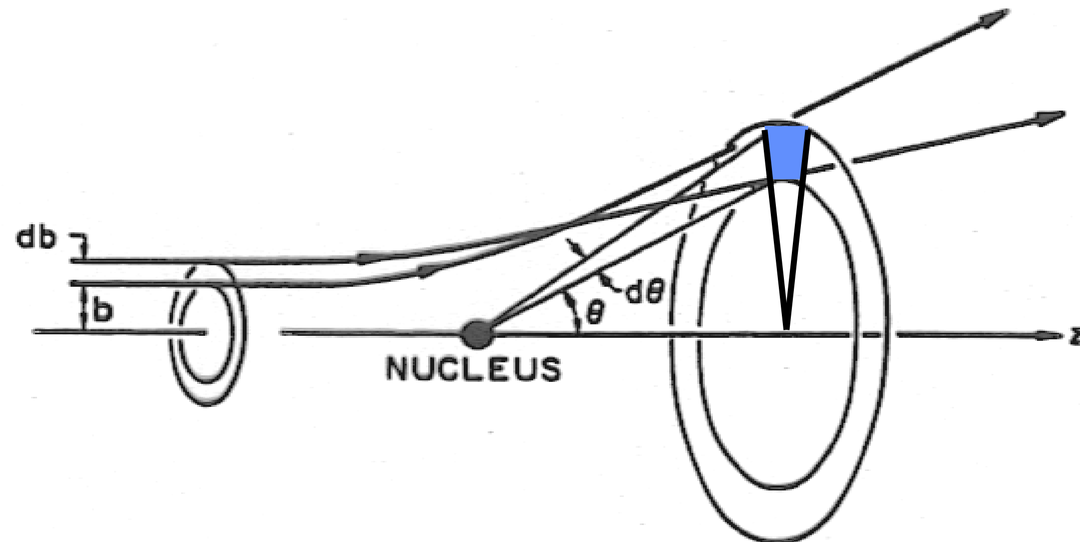

Rutherford cross-section:

$$\frac{d\sigma}{d\Omega} = \left(\frac{Z_1 Z_2 e^2}{2E_o}\right)^2 \frac{\left[\cos\theta + (1 - A^2 \sin^2\theta)^{1/2}\right]^2}{\sin^4\left(\frac{\theta}{2}\right)(1 - A^2 \sin^2\theta)^{1/2}} \qquad A = \frac{m_1}{m_2}$$

Scattering Yield

$$Yield, Y \propto \sigma(\theta) = \left(\frac{Z_1 Z_2 e^2}{2E_0}\right)^2 \frac{\left[\cos\theta + \left(1 - A^2 \sin^2\theta\right)^{1/2}\right]^2}{\sin^4\frac{\theta}{2}\left(1 - A^2\sin^2\theta\right)^{1/2}}$$

$$\propto \left(\frac{Z_1 Z_1}{E_0}\right)^2 \sim 10^{-24} cm^2 [barn]$$

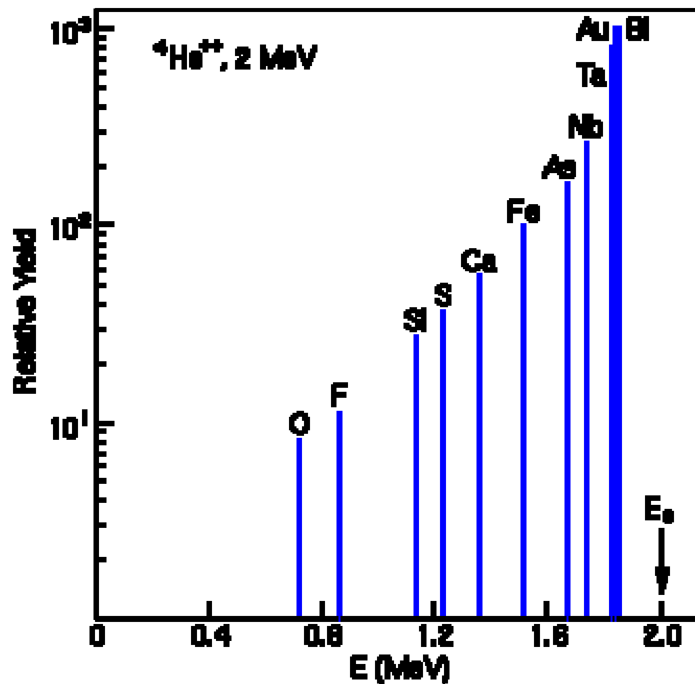

Example:

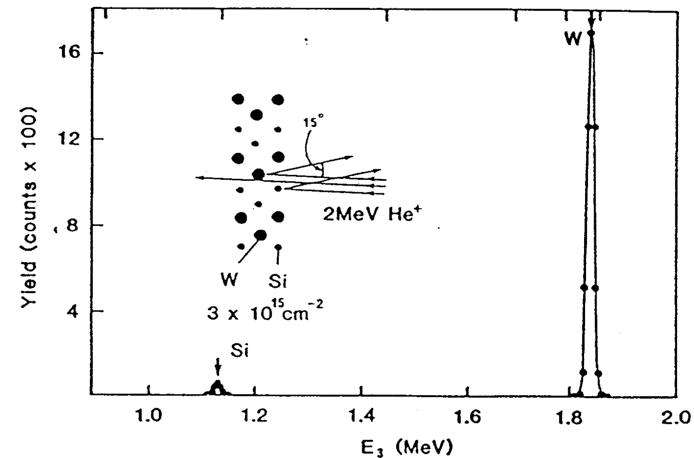

Mixed Si and W target analzed by a 2MeV He ion beam at 165° scattering angle.

σ(Si)=2.5x10^{-25}cm^2/str

σ(W)=7.4x10^{-24}cm^2/str

Total incident ions Q=1.5x10^{14} ions

Ω=1.8mstr

Area under Si, A(Si)=200 counts

Area under W, A(W)=6000 counts

$(Nt)_{Si}$=3x10^{15}atoms/cm^2

$(Nt)_{W}$=3x10^{15}atoms/cm^2

Deviation from Rutherford scattering

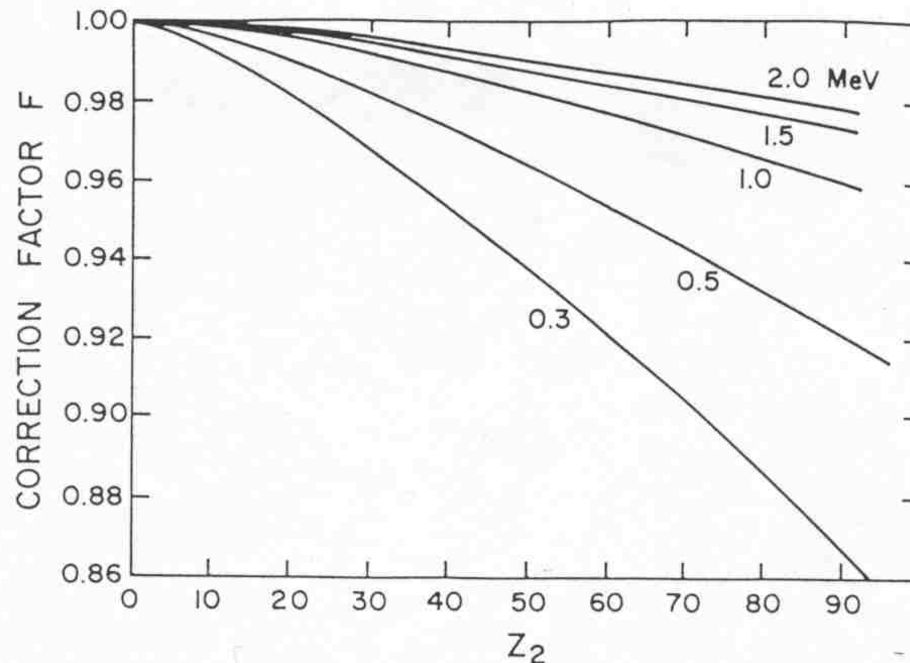

Correction factor F, which describes the deviation from pure Rutherford scattering due to electron screening for He^+ scattering from atoms, Z_2, at variety of incident kinetic energies.

At very high energy and very low energy, scattering will deviate from the Rutherford type.

At low energy : screening of e^- must be considered

At high energy : nuclear short range force will enhance the cross-section, the so-called "resonance scattering."

Energy Loss

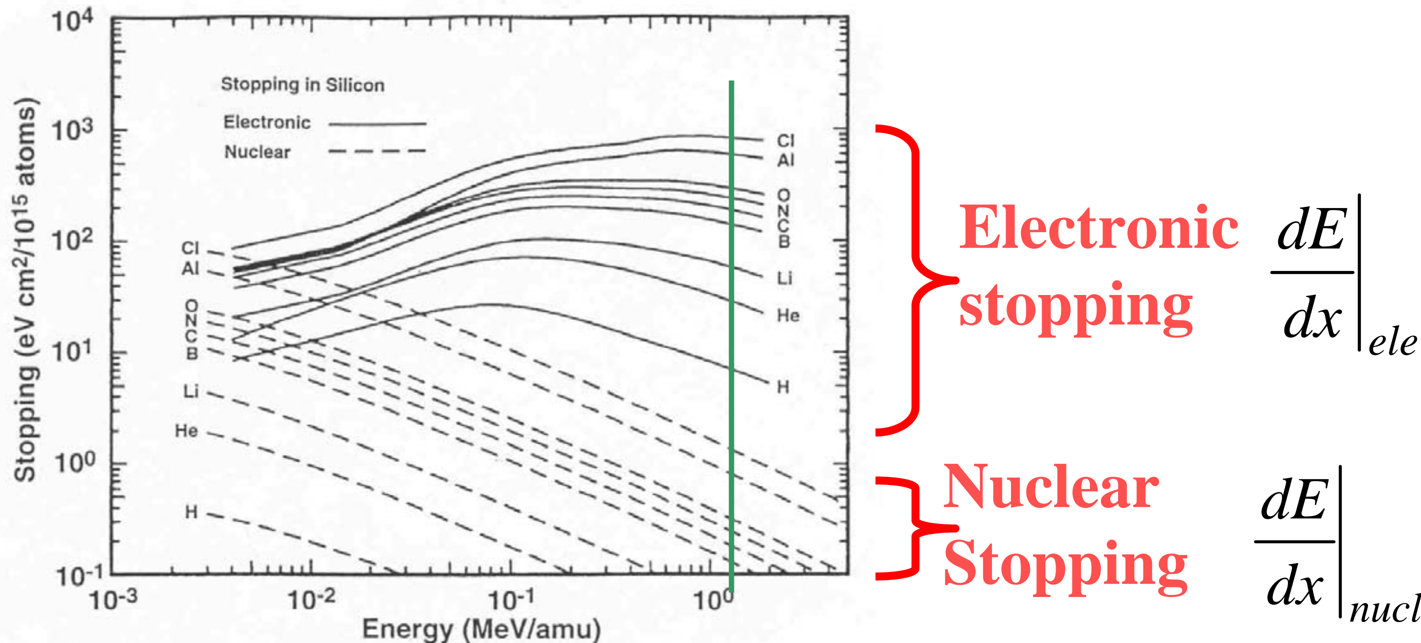

When an He or H ion moves through matter, it loses energy through

- interactions with e⁻ by raising them to excited states or even ionizing them.
- Direct ion-nuclei scattering

Since the radii of atomic nuclei are so small, interactions with nuclei may be neglected

$$\left.\frac{dE}{dx}\right|_{total} = \left.\frac{dE}{dx}\right|_{ele} + \left.\frac{dE}{dx}\right|_{nucl} \approx \left.\frac{dE}{dx}\right|_{ele}$$

How to read a typical RBS spectrum

A thin film on a light substrate

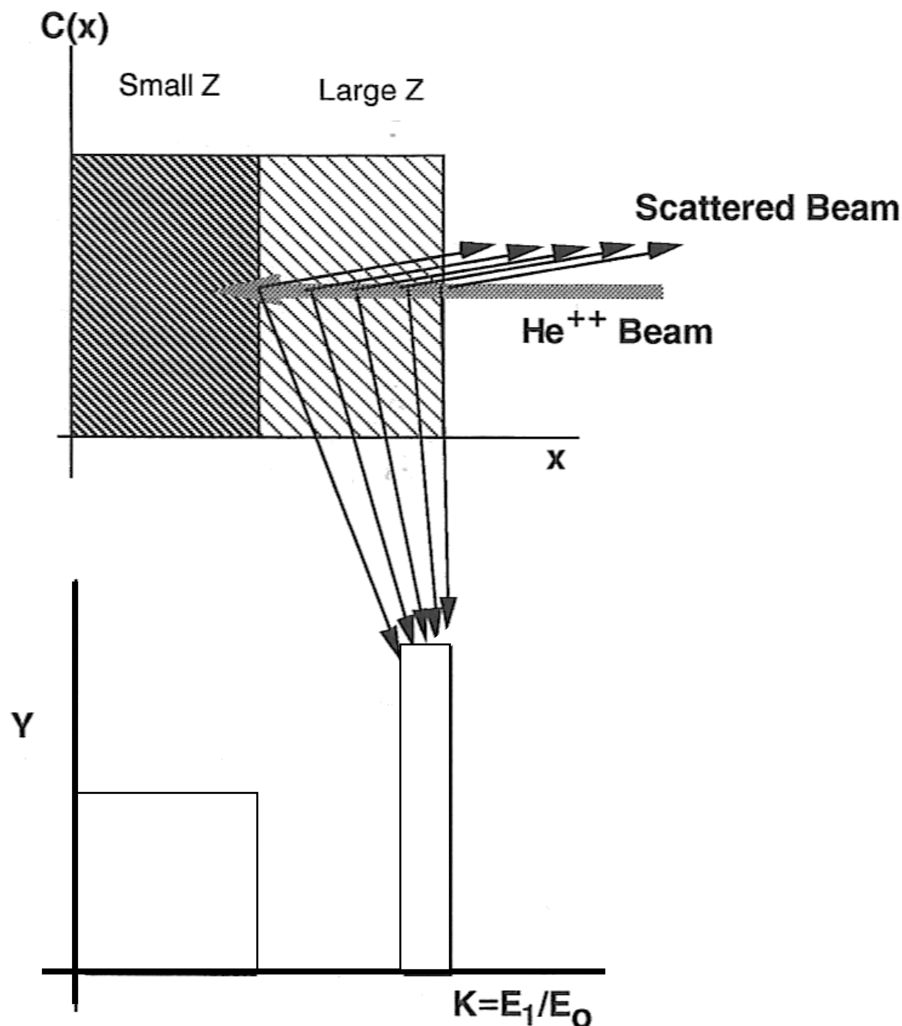

- Most projectile ions experience electronic stopping that results in a gradual reduction of the particle's kinetic energy (dE/dx).
- At the same time a small fraction of projectile ions come close enough to the nucleus for large-angle scattering (KE).
- A detected backscattered particle has lost some energy during initial penetration, then lost a large fraction of its remaining energy during the large-angle scattering event, then lost more energy in leaving the solid.

Depth Scale

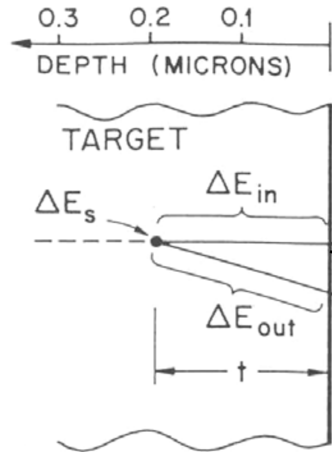

ENERGY LOSS:

$$\Delta E_{in} \simeq \left.\frac{dE}{dx}\right|_{E_0} \cdot t$$

$$E_t = E_0 - \Delta E_{in}$$

$$\Delta E_s = (1-K)\,E_t$$

$$\Delta E_{out} \simeq \left.\frac{dE}{dx}\right|_{E_1} \cdot \frac{t}{\cos\theta}$$

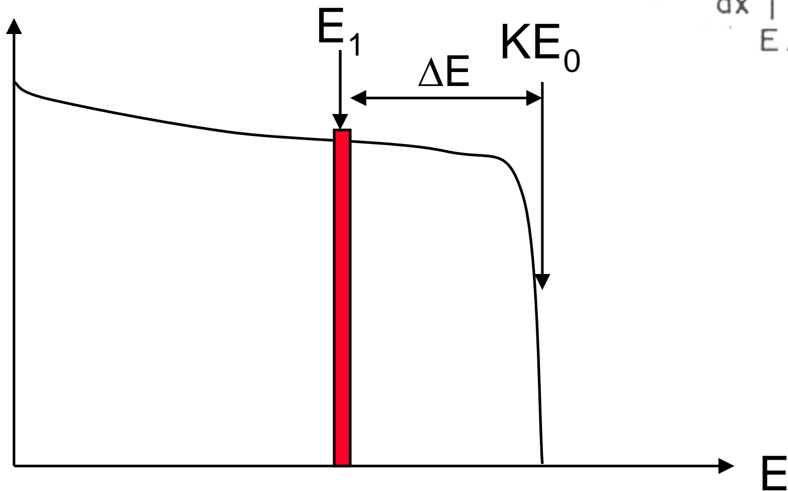

$$E_1 = K(E_0 - \Delta E_{in}) - \Delta E_{out}$$

$$E_1 = K\left(E_0 - \left.\frac{dE}{dx}\right|_{E_0} \bullet t\right) - \left(\left.\frac{dE}{dx}\right|_{KE_0} \bullet \frac{t}{\cos\theta}\right)$$

Total energy loss $\Delta E = KE_0 - E_1$

$$\Delta E = \left(\frac{K}{\cos\theta_1} \bullet \left.\frac{dE}{dx}\right|_{E_0} + \frac{1}{\cos\theta_2} \bullet \left.\frac{dE}{dx}\right|_{KE_0}\right) \bullet t = [S_o] \bullet t$$

$[S_o]$ is the effective stopping power

Stopping cross-section

$$\varepsilon = \frac{1}{N}\frac{dE}{dx} : \frac{\text{eV}}{\text{cm}}\frac{\text{cm}^3}{\text{atom}} = \frac{\text{eVcm}^2}{\text{atom}}$$

$$\Delta E = \left(\frac{K}{\cos\theta_1} \bullet N\varepsilon_{in} + \frac{1}{\cos\theta_2} \bullet N\varepsilon_{out}\right) \bullet t = N[\varepsilon_o] \bullet t$$

Depth scale: thin film

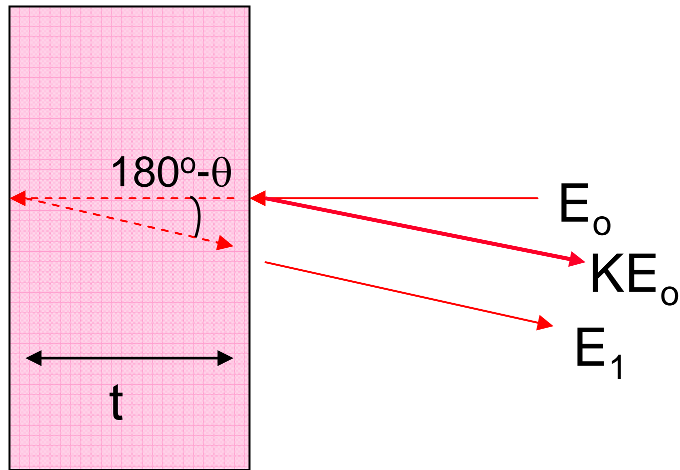

Thickness of film:

$$\Delta E = \left(K\frac{dE}{dx}\bigg|_{E_0} + \frac{\frac{dE}{dx}\big|_{KE_0}}{\cos\theta}\right)\bullet t = [S_o]\bullet t$$

$$t = \frac{\Delta E}{[S_o]} = \frac{\Delta E}{N[\varepsilon_o]}$$

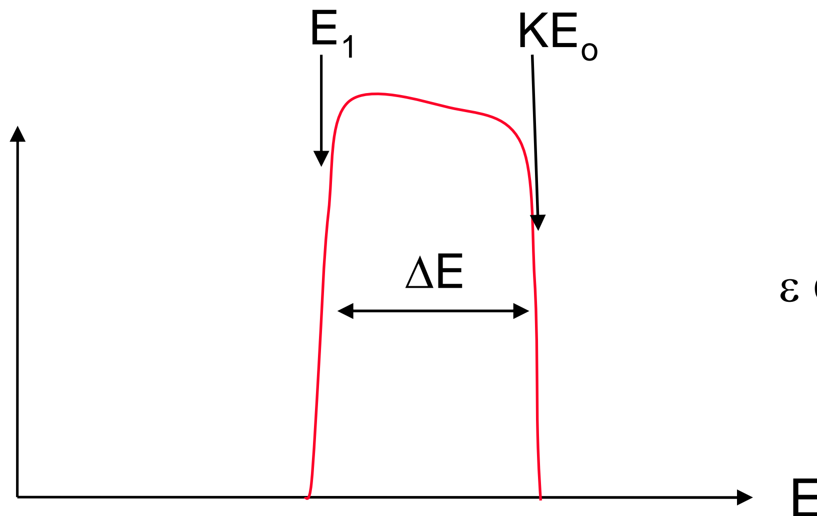

ε obtained from TRIM code or empirical energy loss data fitting

Example: layer thickness

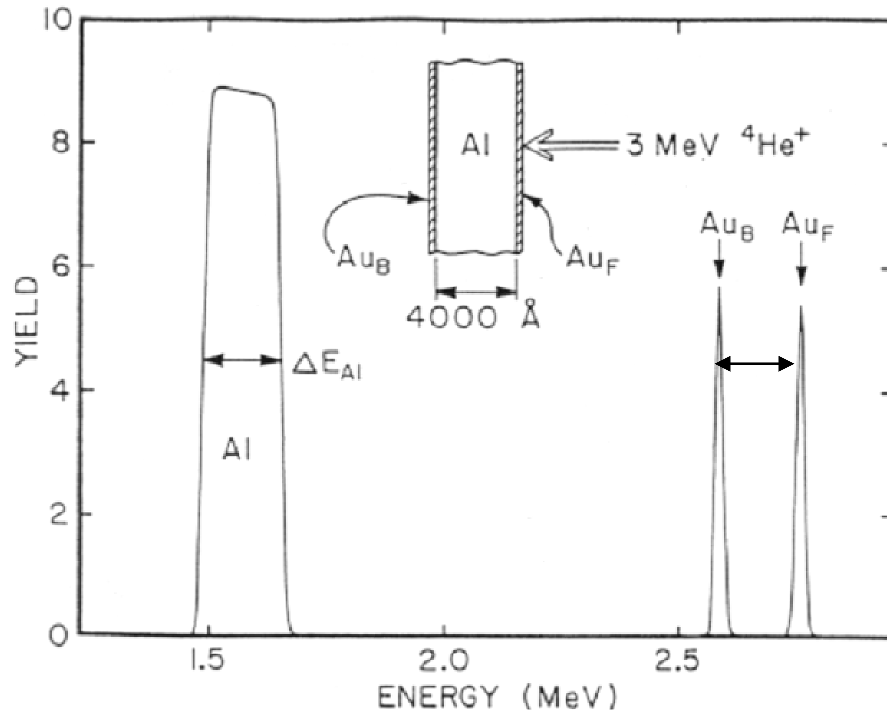

ΔE_{Al} = 165keV

ΔE_{Au} = 175keV

K_{Au} = 0.9225

K_{Al} = 0.5525

consider the Au markers

$\Delta E_{Au} = E_{AuF} - E_{AuB}$

$= [K_{Au}\, dE/dx|_{Eo} + 1/(\cos 10^o) \bullet dE/dx|_{EAuB}] \bullet t$

$dE/dx|_{3MeV} = N_{Al}\, \varepsilon_{Al}|_{3MeV}$

$= 6.02x10^{22} \bullet 36.56x10^{-15}$

$= 2.2x10^{9} eVcm^{-1}$

$dE/dx|_{EAuB} = N_{Al}\, \varepsilon_{Al}|_{2.57MeV}$

$= 6.02x10^{22} \text{ x } 39.34x10^{-15}$

$= 2.37x10^{9}\ eVcm^{-1}$

t = 3945Å

consider the Al signals

$\Delta E_{Al} = [K_{Al}\, dE/dx|_{Eo} + 1/(\cos 10^o) \bullet dE/dx|_{KEo}] \bullet t$

t = 3937Å

Energy Loss: Bragg's rule

For a target A_mB_n, the stopping cross-section is the sum of those of the constituent elements weighted by the abundance of the elements.

$$\varepsilon^{AmBn} = m\,\varepsilon^{A} + n\,\varepsilon^{B}$$

Example:

the stopping cross-section ε^{Al2O3} of Al_2O_3.

Given: $\varepsilon^{Al} = 44 \times 10^{-15}$eVcm^2

$\varepsilon^{O} = 35 \times 10^{-15}$eVcm^2

$\varepsilon^{Al2O3} = 2/5 \times \varepsilon^{Al} + 3/5 \times \varepsilon^{O}$

$= (2/5 \times 44 + 3/5 \times 35) \times 10^{-15}$

$= 38.6 \times 10^{-15}$ eV-cm^2/atom

$dE/dx(Al_2O_3) = N\varepsilon^{Al2O3} = (1.15\times10^{22})(38.6\times10^{-15})$eV/cm

$=44.4$ eV/Å

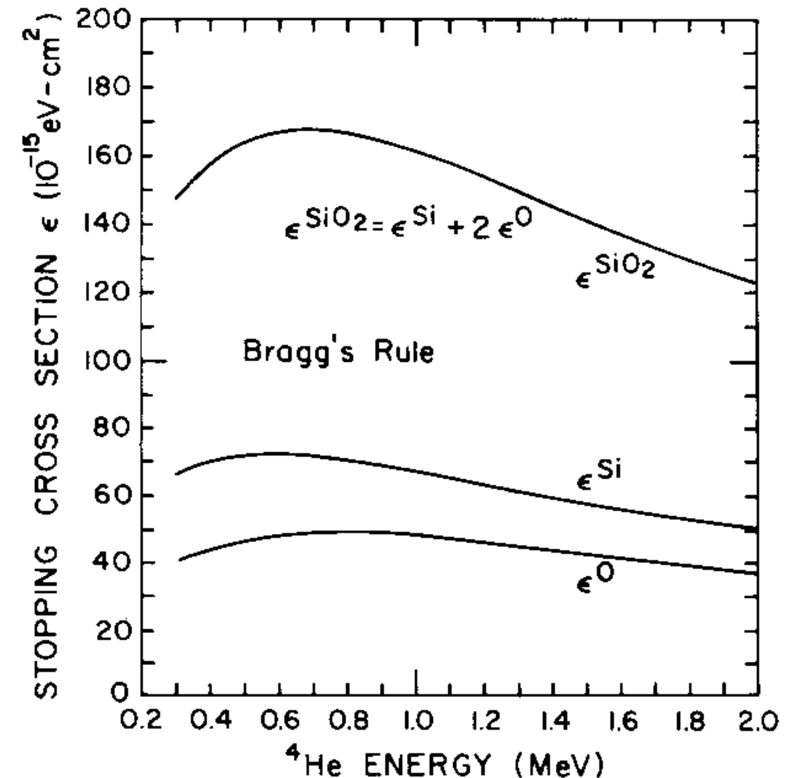

Quantitative analysis: composition and thickness

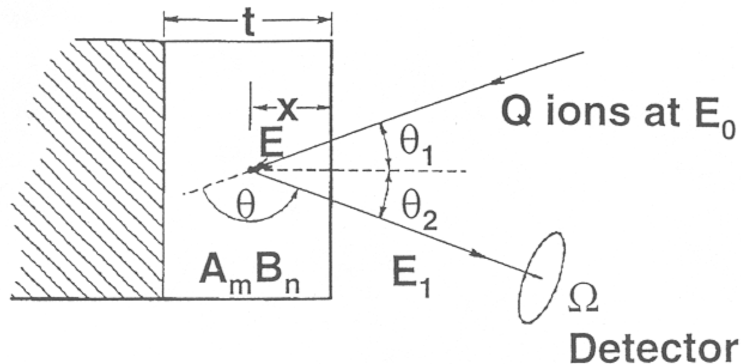

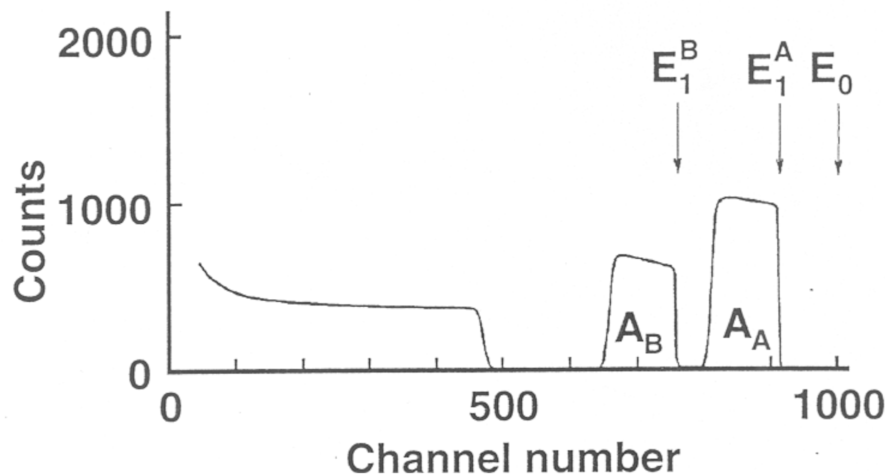

$A_A = \sigma_A \bullet \Omega \bullet Q \bullet (Nt)_A$

$A_B = \sigma_B \bullet \Omega \bullet Q \bullet (Nt)_B$

$$\frac{A_A}{A_B} = \left(\frac{\sigma_A}{\sigma_B}\right) \bullet \left(\frac{(Nt)_A}{(Nt)_B}\right) = \left(\frac{Z_A}{Z_B}\right)^2 \bullet \frac{m}{n}$$

$$\frac{m}{n} = \left(\frac{A_A}{A_B}\right) \bullet \left(\frac{Z_B}{Z_A}\right)^2$$

$$t = \frac{(\Delta E)_A}{[S_o]_A^{A_m B_n}} = \frac{(\Delta E)_B}{[S_o]_B^{A_m B_n}}$$

$$t = \frac{(\Delta E)_A}{N[\varepsilon_o]_A^{A_m B_n}} = \frac{(\Delta E)_B}{N[\varepsilon_o]_B^{A_m B_n}}$$

Example: As implanted Si

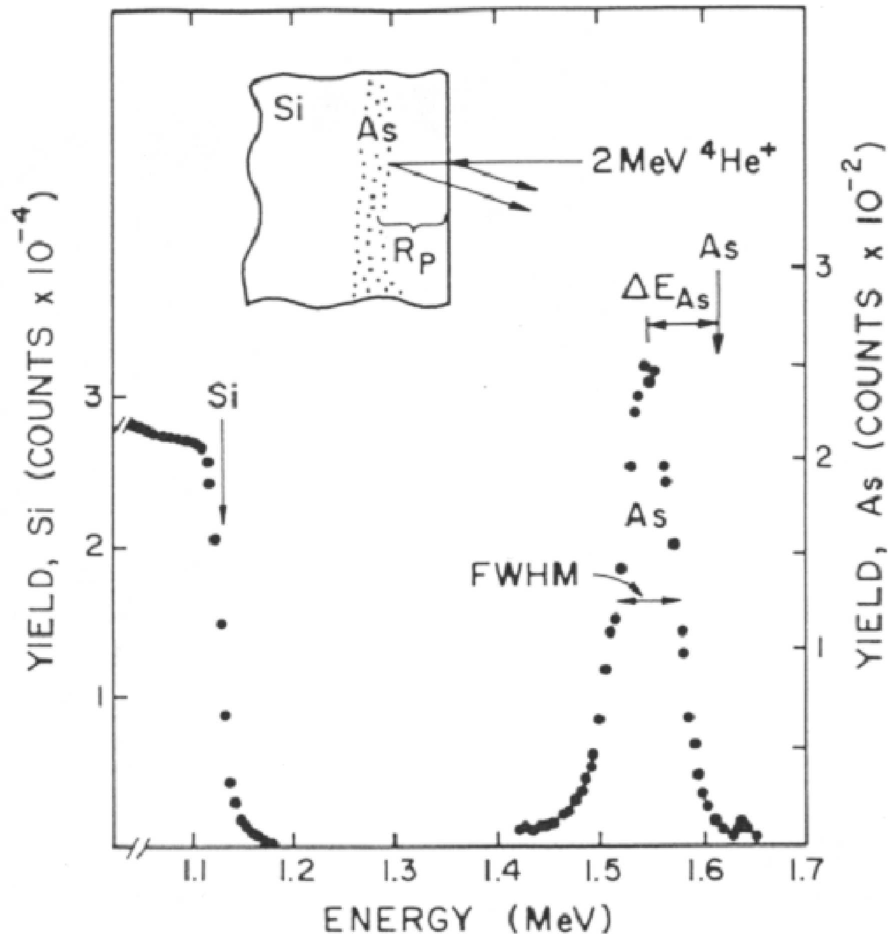

K_{As}=0.809; K_{Si}=0.566

$$[\varepsilon_o]_{Si}^{Si} = 92.6x10^{-15} eV - cm^2 / atom$$

$$[\varepsilon_o]_{As}^{Si} = 95.3x10^{-15} eV - cm^2 / atom$$

$$\Delta E_{As}^{Si} = 68keV$$

$$(FWHM)_{As} = 60keV$$

$$R_p = \frac{\Delta E_{As}^{Si}}{N[\varepsilon_o]_{As}^{Si}} = 1420\text{Å}$$

$$\Delta R_p = \frac{(FWHM)_{As}}{2.355 \bullet N[\varepsilon_o]_{As}^{Si}} = 540\text{Å}$$

Total As dose:

$$(Nt)_{As} = \frac{A_{As}}{(\sigma_{As} \bullet \Omega \bullet Q)}$$

Quantitative Analysis

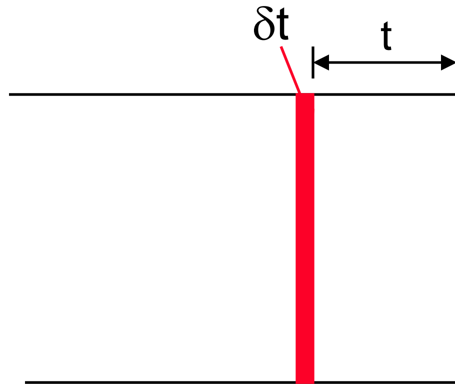

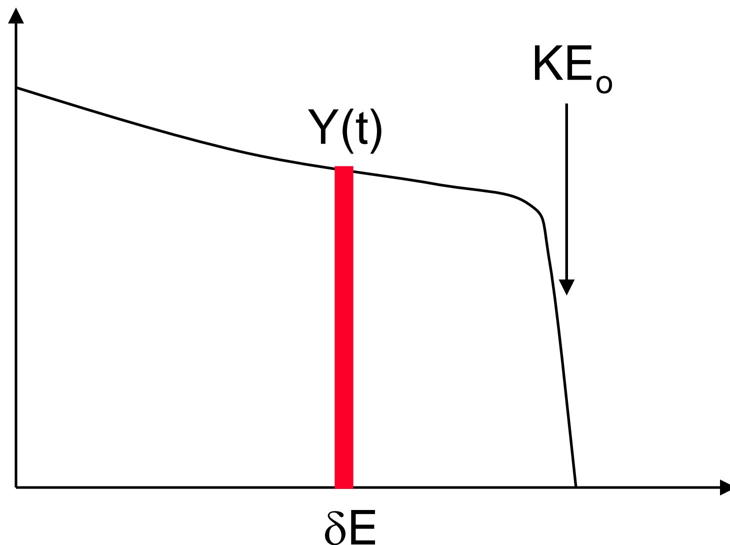

When Y(t) corresponds to the yield for one energy division in the RBS spectrum:

$Y(t)=H(E)$

$H(E)=\sigma\bullet\Omega\bullet Q\bullet N\bullet\delta t$

$\quad=\sigma\bullet\Omega\bullet Q\bullet N\bullet\delta E/[S_o]$

$\quad=\sigma\bullet\Omega\bullet Q\bullet N\bullet\delta E/N[\varepsilon_o]$

where δE is the energy/channel in the RBS spectrum

Consider the As implanted Si example:

$A_{As}=\sigma_{As}\bullet\Omega\bullet Q\bullet(Nt)_{As}$

$$H_{Si}=\sigma_{Si}\bullet\Omega\bullet Q\bullet N\frac{\delta E}{N[\varepsilon_o]_{Si}^{Si}}$$

$$\frac{As_{As}}{H_{Si}}=(\frac{Z_{As}}{Z_{Si}})^2\bullet\frac{(Nt)_{As}}{\delta E/[\varepsilon_o]_{Si}^{Si}}$$

Independent of Q and Ω

Thin film analysis

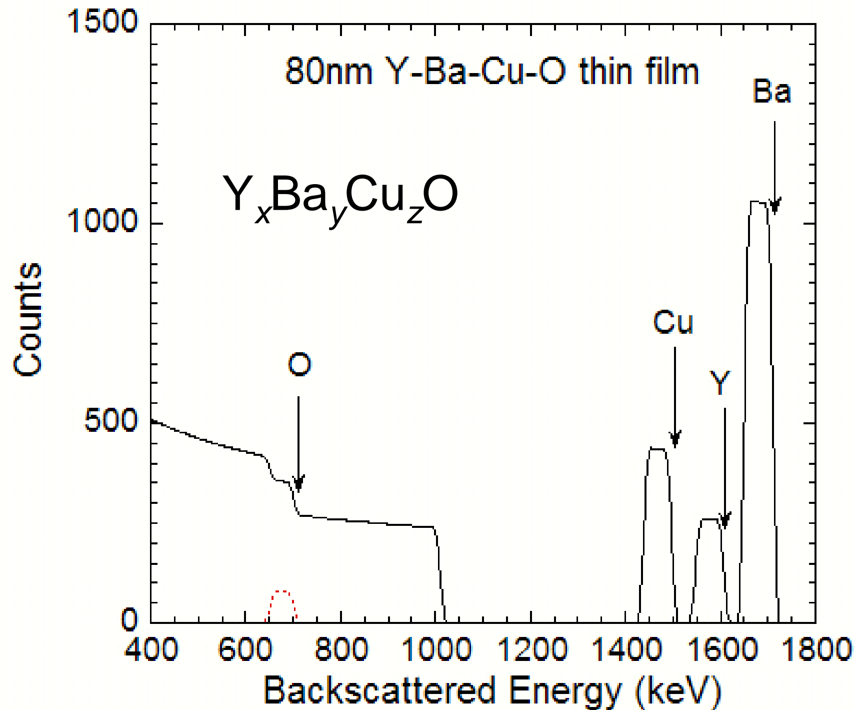

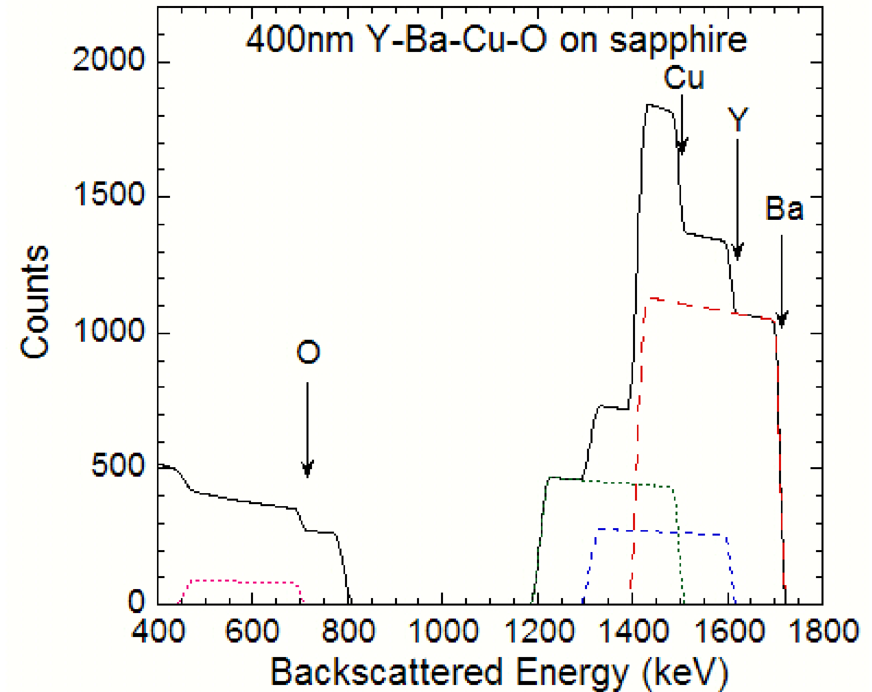

$$\frac{y}{x} = \frac{A_Y}{A_{Ba}} \bullet \left(\frac{Z_{Ba}}{Z_Y}\right)^2$$

$$\frac{y}{x} = \frac{H_Y}{H_{Ba}} \bullet \left(\frac{Z_{Ba}}{Z_Y}\right)^2 \bullet \frac{[\varepsilon_o]_Y^{YBCO}}{[\varepsilon_o]_{Ba}^{YBCO}}$$

$$\approx \frac{H_Y}{H_{Ba}} \bullet \left(\frac{Z_{Ba}}{Z_Y}\right)^2$$

RBS simulation

La-Sr-Mn-O on Si

La-Sr-Mn-O

Si

$^4He^+$

O

Mn

Sr

La

Counts

1500
1000
500
0

600 800 1000 1200 1400 1600 1800

Backscattered Energy (keV)

Example: silicide formation

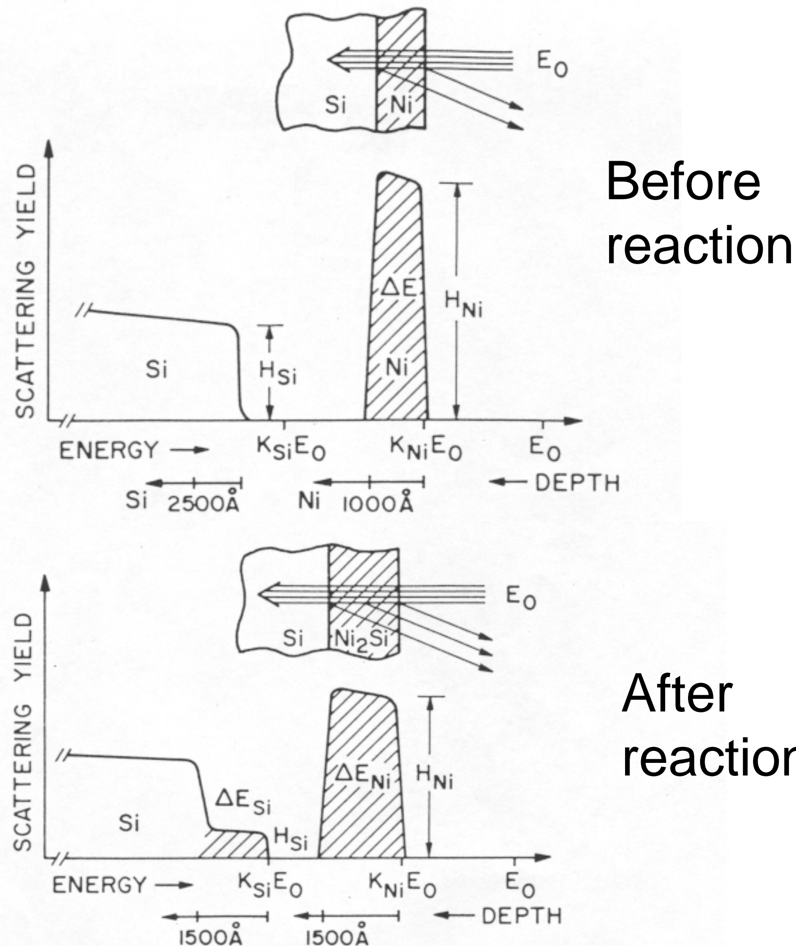

Figure 3.10 Schematic backscattering spectra for MeV ^4He ions incident on 1000 Å Ni film on Si *(top)* and after reaction to form Ni_2Si *(bottom)*. Depth scales are indicated below the energy axes.

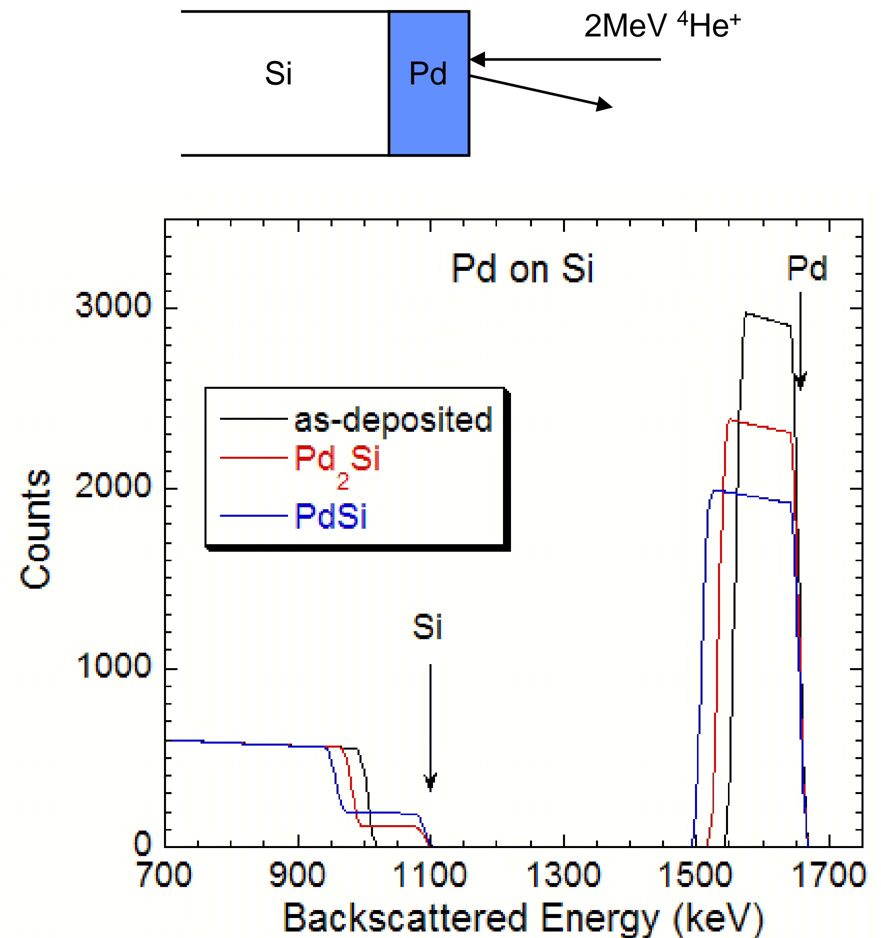

RBS application: silicide formation

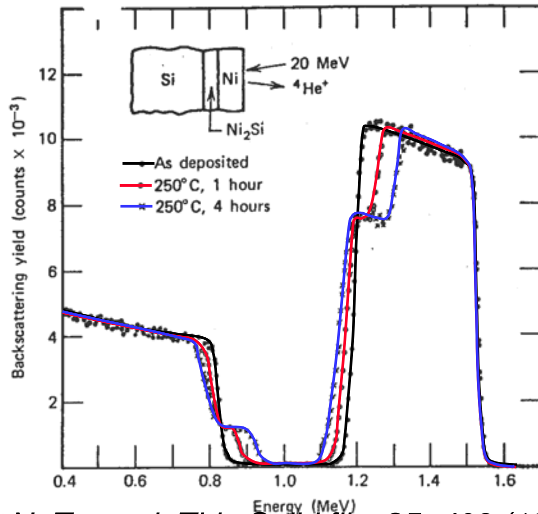

K. N. Tu et al. Thin Solid film ***25****, 403 (1975).*

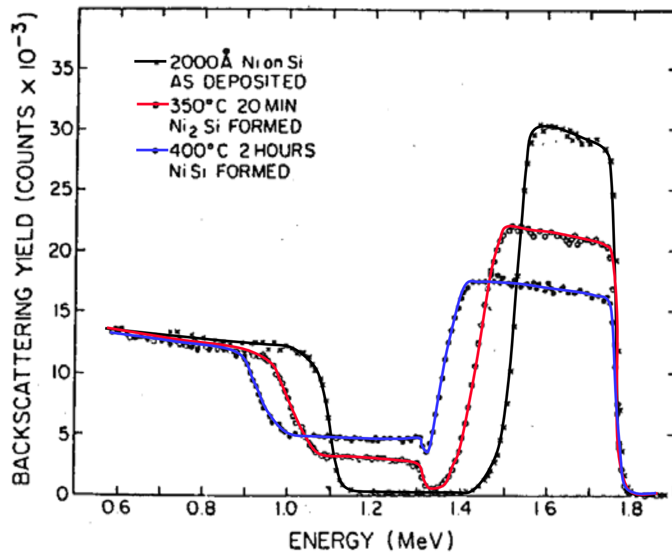

K. N. Tu et al. Japn, J. Appl. Phys. Suppl. ***2*** *Pt 1 669 (1974).*

Reaction kinetics:

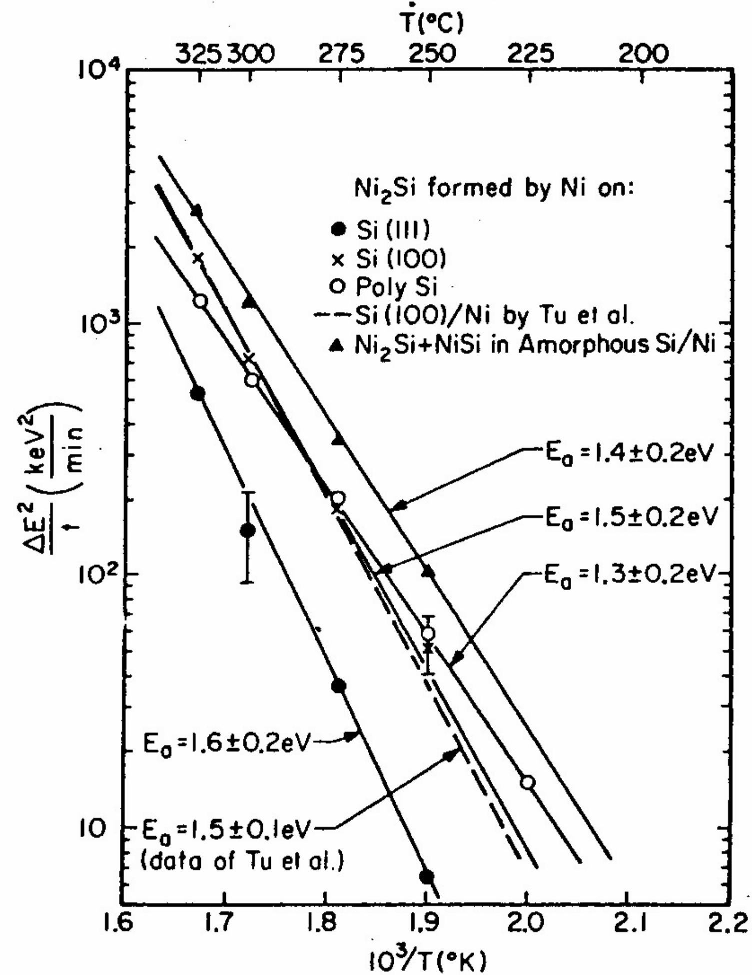

J. O. Olowolafe et al. Thin Solid film ***38****, 143 (1976).*

RBS Application: impurity profile

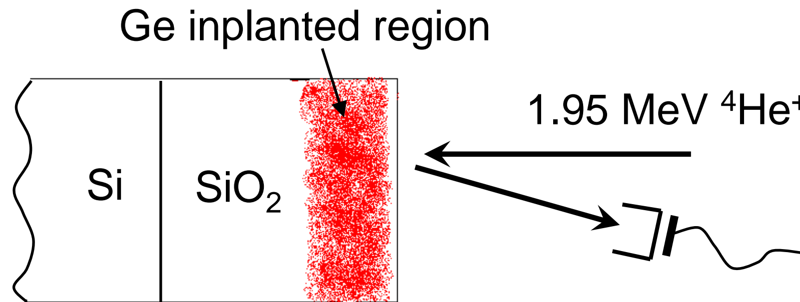

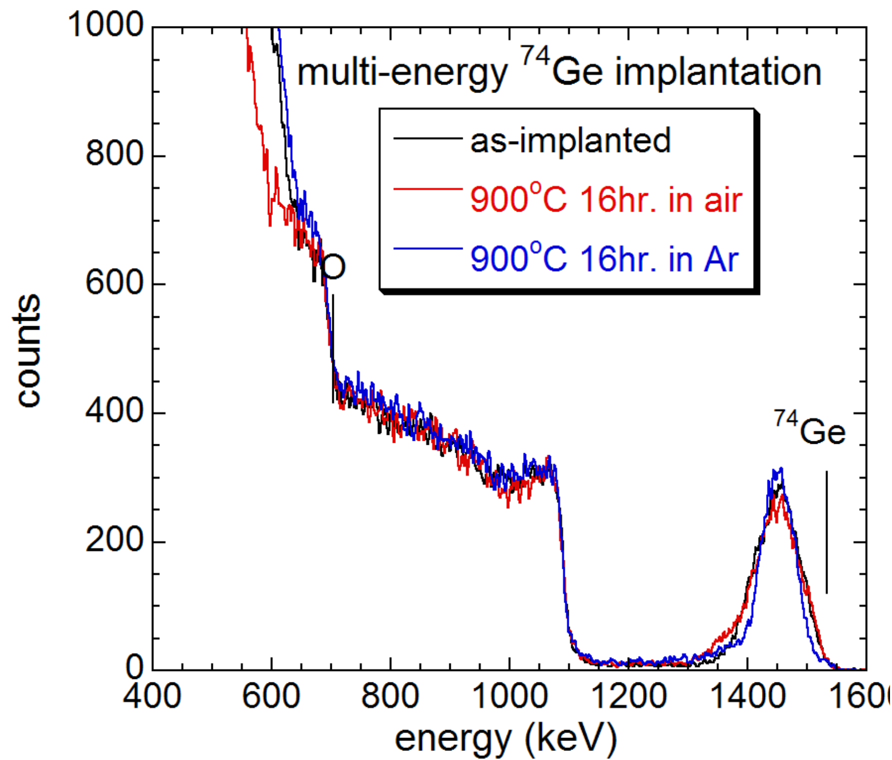

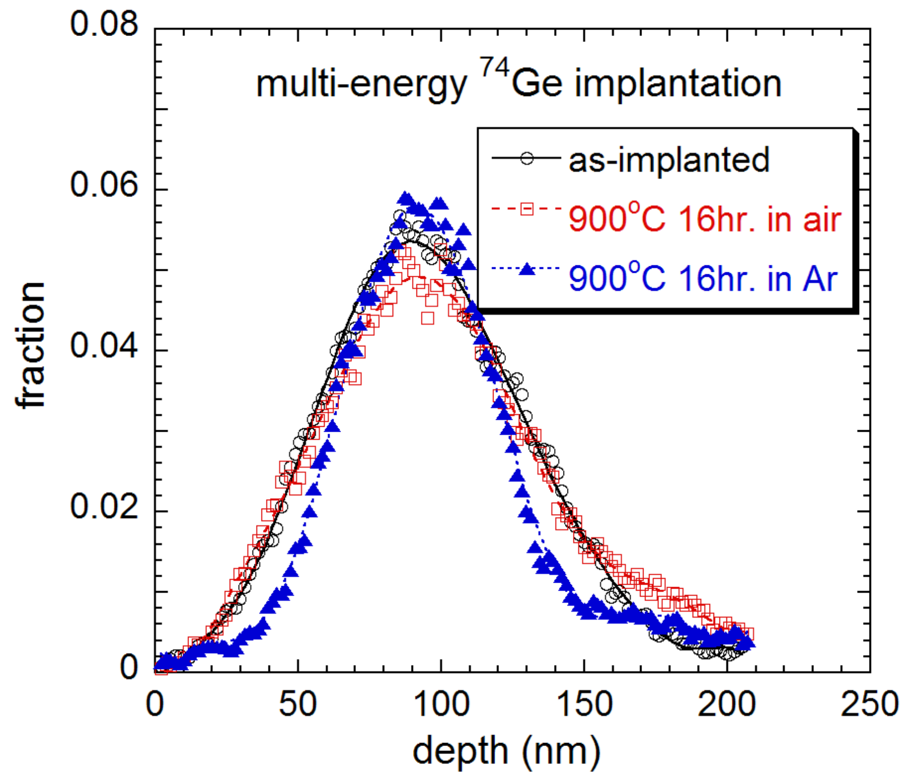

I. Sharp et al., LBNL (2004)

Pitfalls in IBA

- **Charge Integration**
  - Accurate charge integration is important for absolute quantitative measurements
    - Good faraday cup design

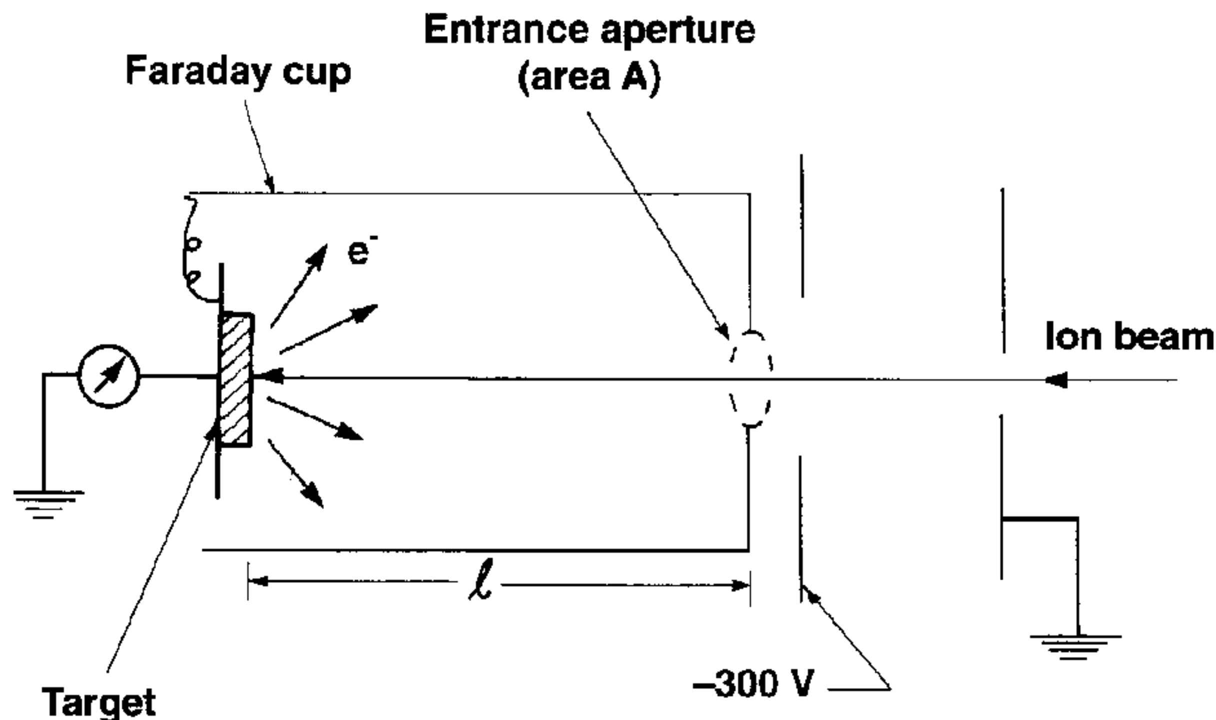

Pitfalls in IBA (cont.)

- Deviation from Rutherford cross-section:

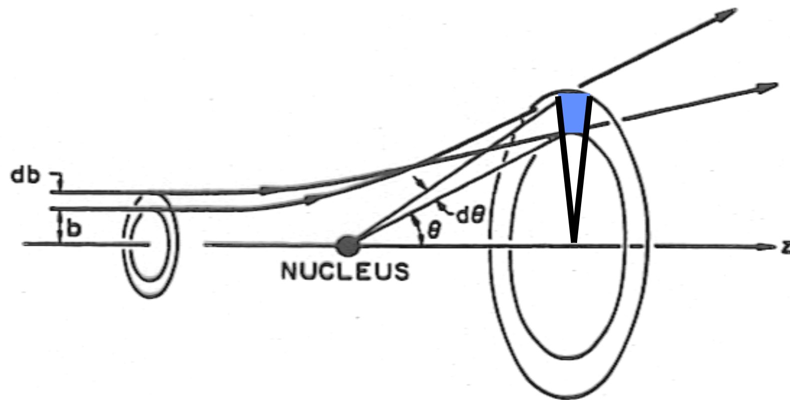

b=distance of closest approach=$Z_1Z_2e^2/E$
r_n= nuclear radius=$1.4Z_2^{1/3}x10^{-5}$
r_K=atomic K-shell radius=$0.5/Z_2$

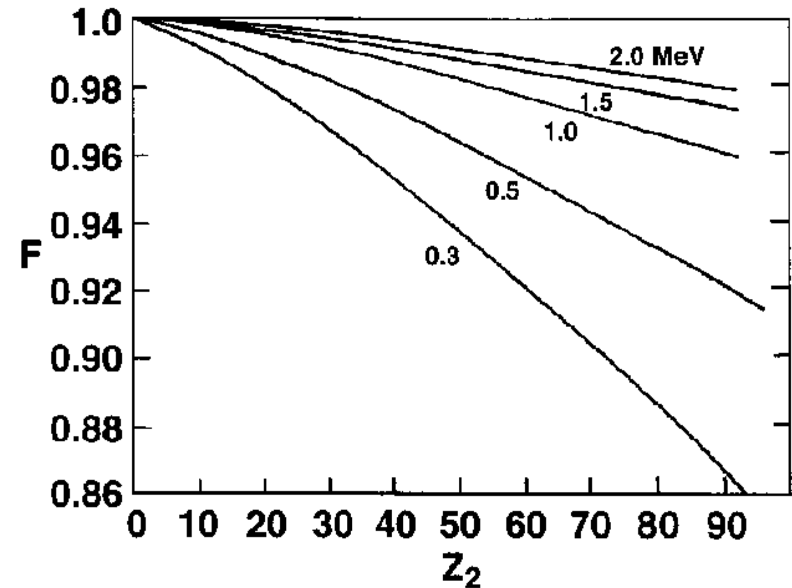

FIG. 12.5. Screening-correction factor, F, to the Rutherford cross section for ^{4}He backscattering as a function of Z_2 and E (L'Ecuyer et al., 1979)

In order to miminize electron screening and maintain a point charge approximation:
$0.5r_K > b > 3r_n$

For typical RBS: Rutherford cross section is valid (~4%)

Pitfalls in IBA (cont.)

- Insulating samples: charging effect

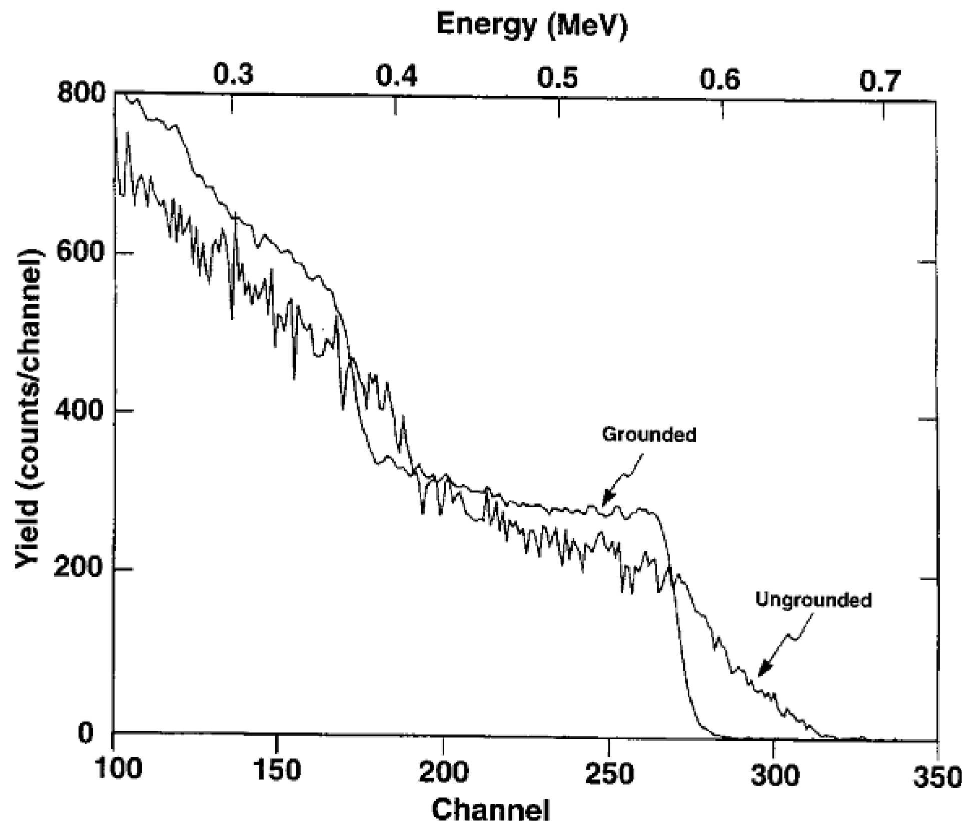

FIG. 12.8. Surface charging effect. Comparison of RBS spectra from a quartz target using 1 MeV ^{4}He: a) ungrounded; b) grounded via a thin conductive surface layer of graphite by rubbing a pencil lightly across the surface (Almeida and Macauley-Newcombe, 1991).

Severely distort the RBS spectrum

- Provide a supply of low-E electrons from a small, hot filament located nearby
- Coating the surface with a very thin layer of conducting material

Pitfalls in IBA (cont.)

- **Target non-uniformity**
  - Surface roughness and interface roughness cannot be distingusihed
  - Target non-uniformity will resemble diffusion

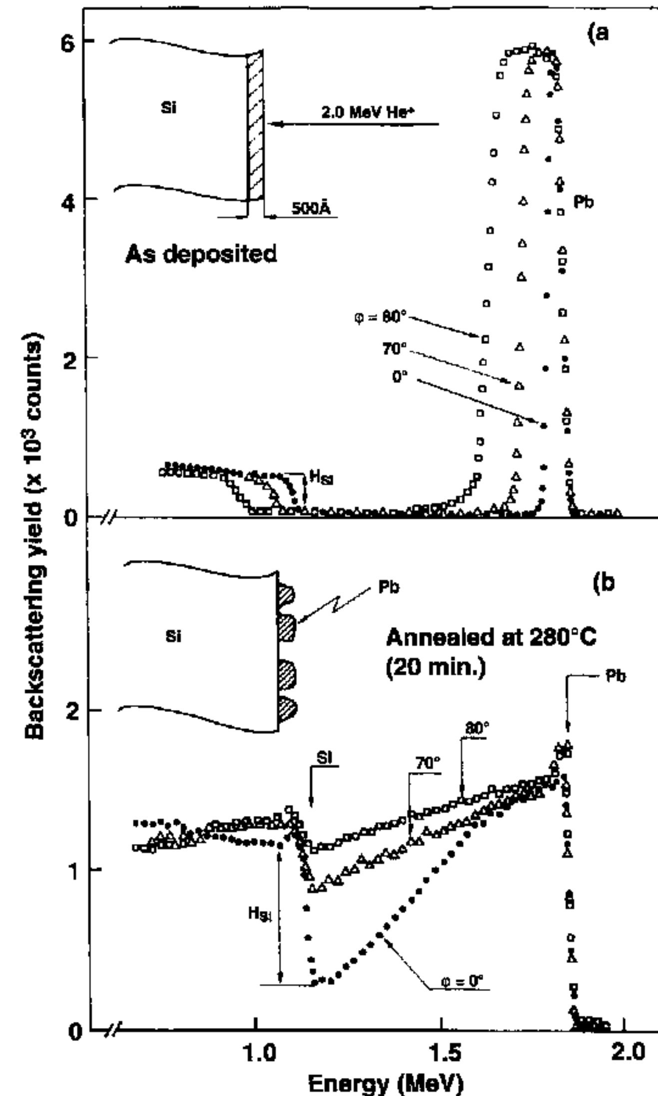

Campisano et al., 1978

Weaknesses of RBS

- Poor lateral resolution (~1mm)
- Moderate depth resolution (~100Å)
- No microstructural information
- No phase identification
- Poor mass resolution for target mass heavier than 70amu
- Detection of light impurities in a heavy matrix difficult (e.g. C, O, B in Si)

Particle Induced X-ray Emission (PIXE)

Paricle Induced X-ray Emission (PIXE)

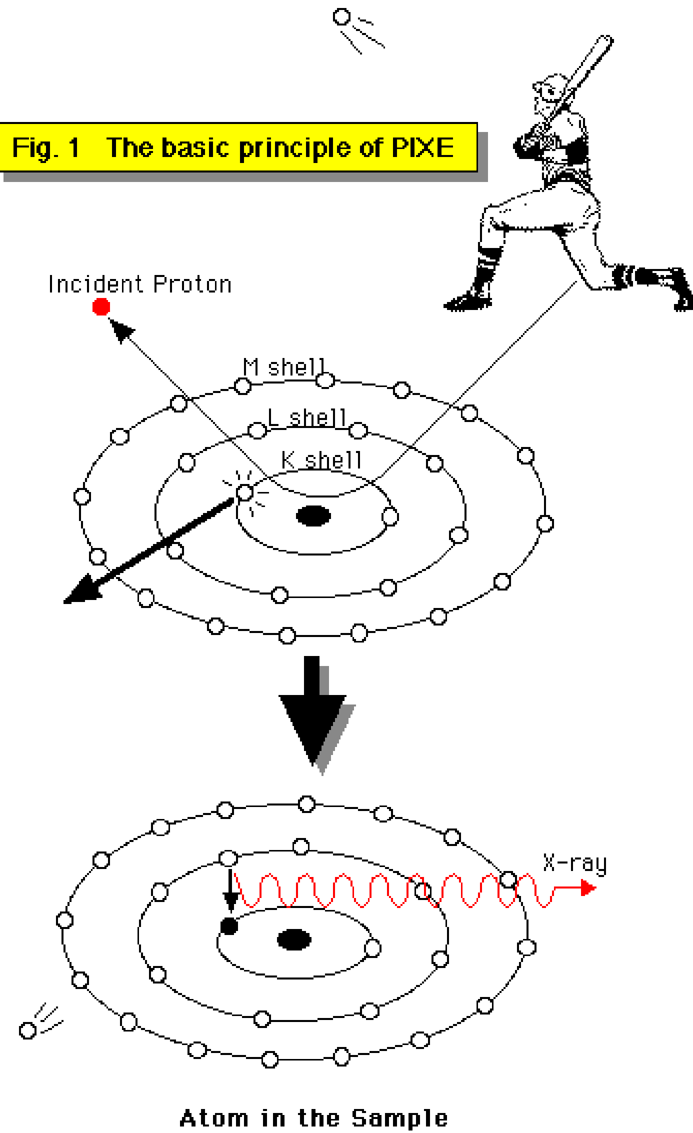

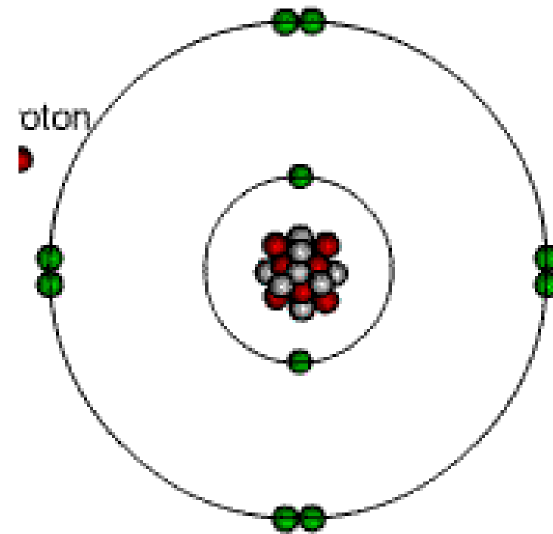

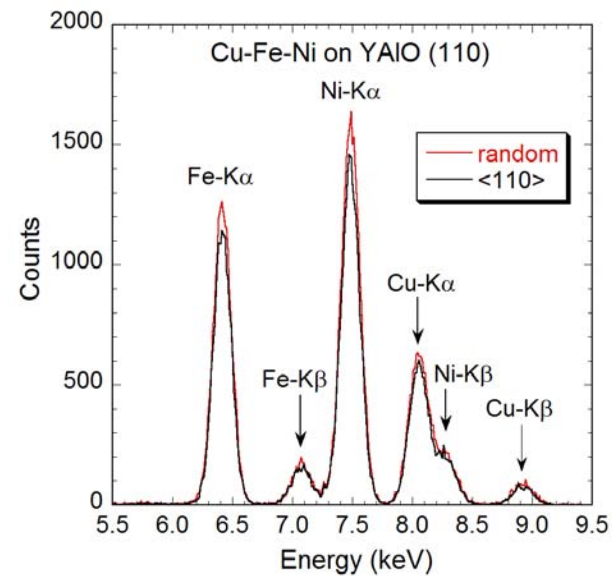

PIXE: Light impurity in heavy matrix

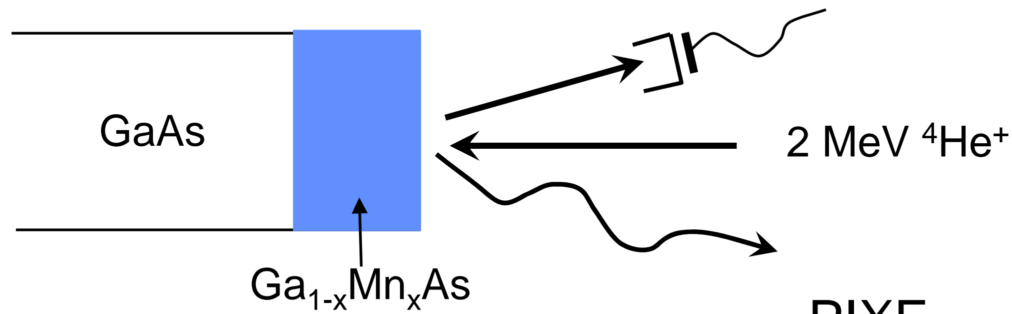

RBS

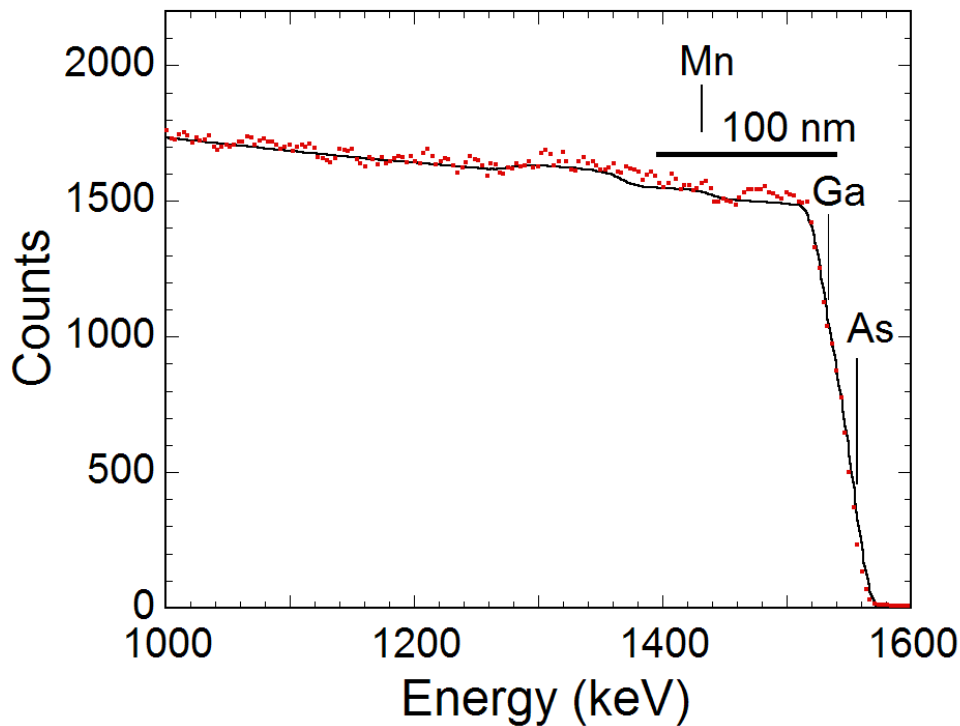

PIXE

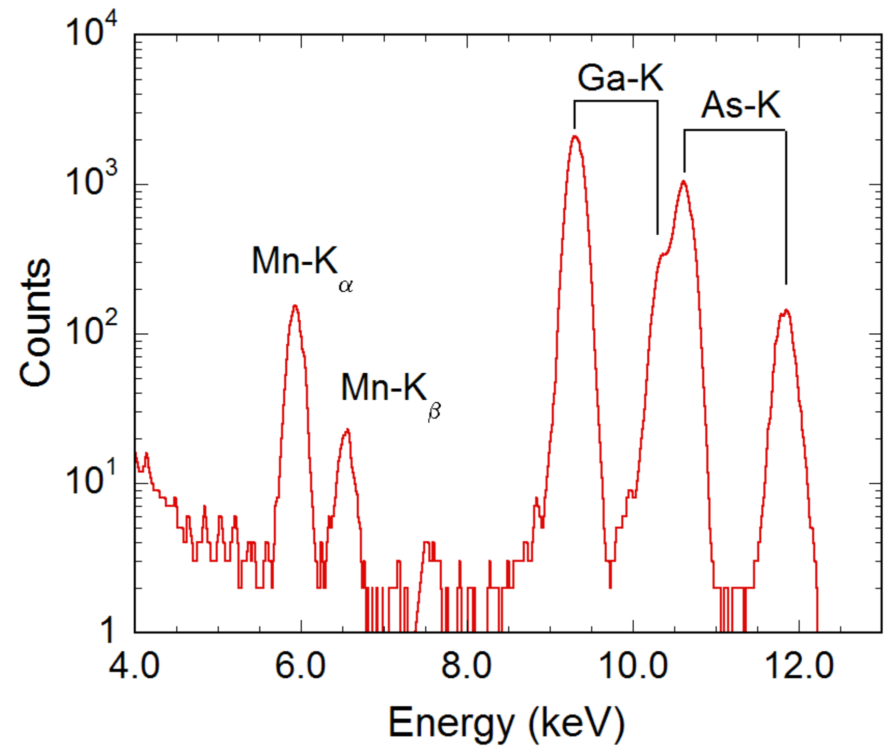

K. M. Yu et al. 2002.

PIXE Application: Geology, Art, Archeology, Biology

External Beam

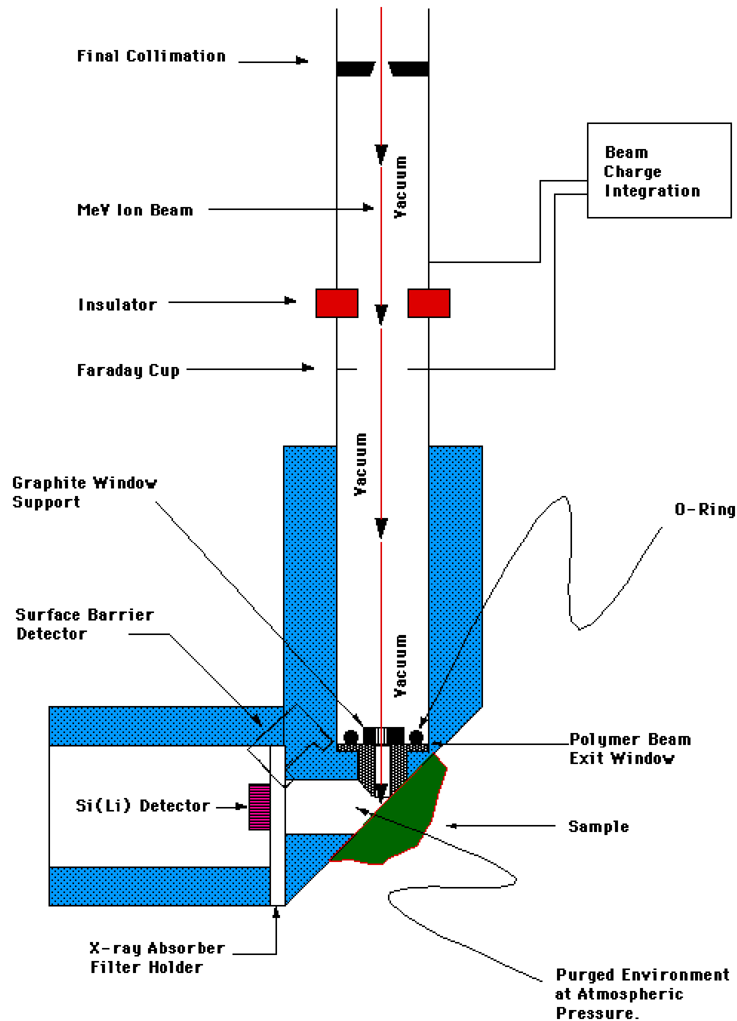

HARVARD PIXE SYSTEM

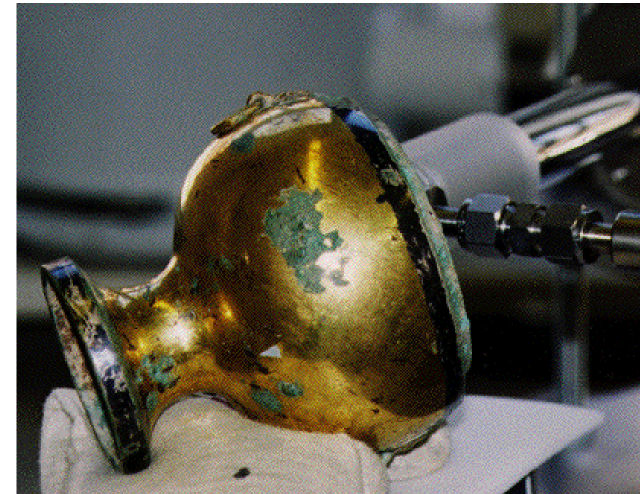

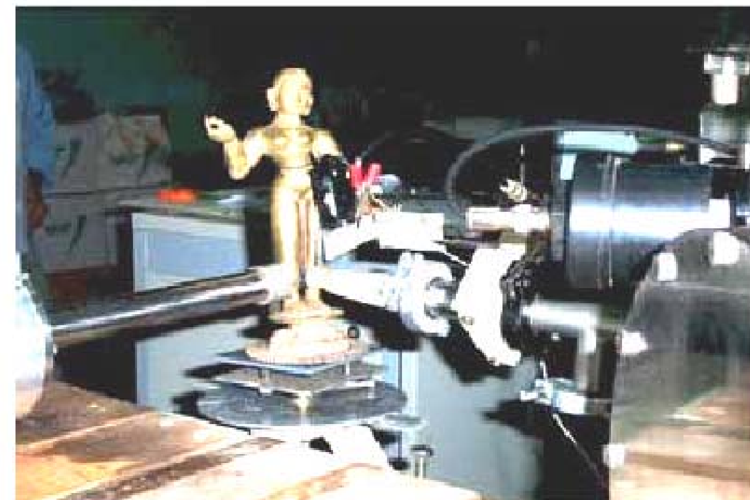

Figure 1. External PIXE set-up at IOP.

Hydrogen Forward Scattering (HFS)
(Elastic Recoil Detection Analsyis ERDA)

Hydrogen Forward Scattering (HFS)

Generally known as Elastic Recoil Detection (ERD)

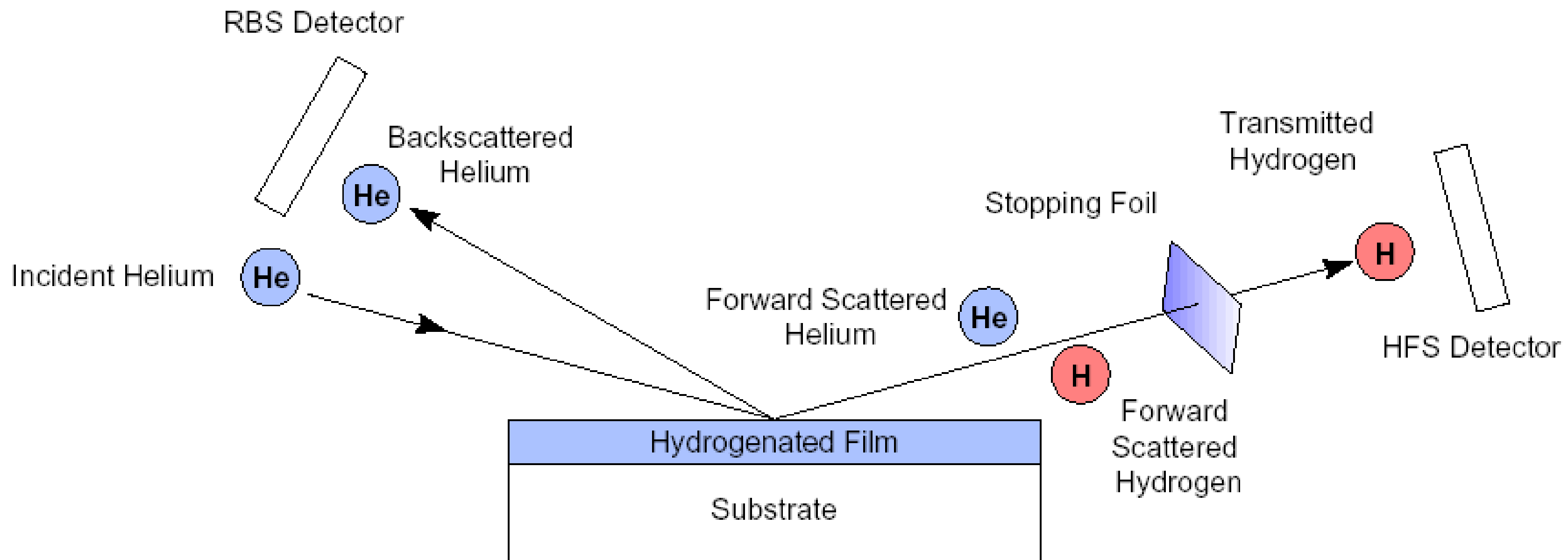

Charles Evans and Assoc., RBS APPLICATION SERIES NO. 3

- Quantitative hydrogen and deuterium profiling
- Good sensitivity (~0.01at% of H)
- Can be perform simultaneously with RBS and PIXE
- Profiling with any light element in solid (using heavy ion beam, ERD)

HFS: H implanted Si

Channeling-RBS

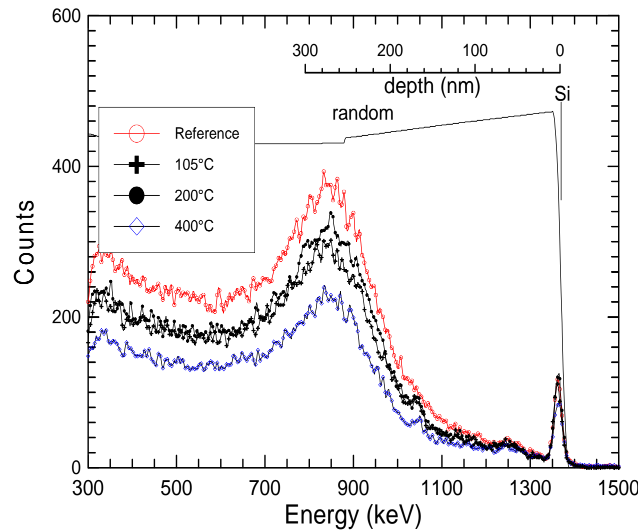

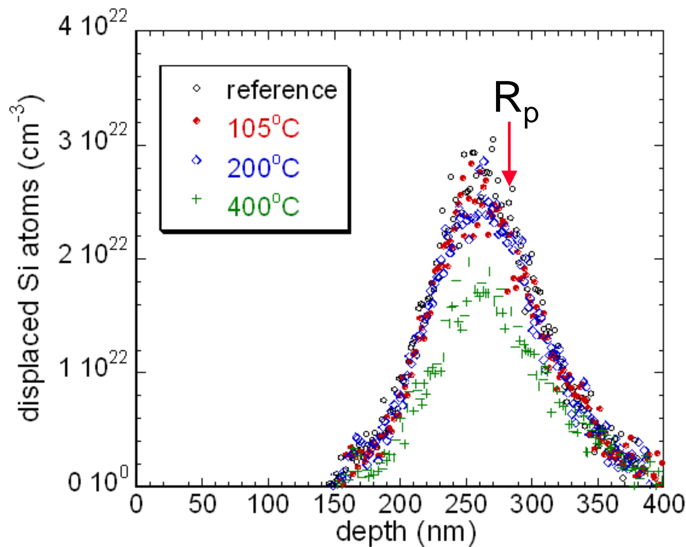

HFS

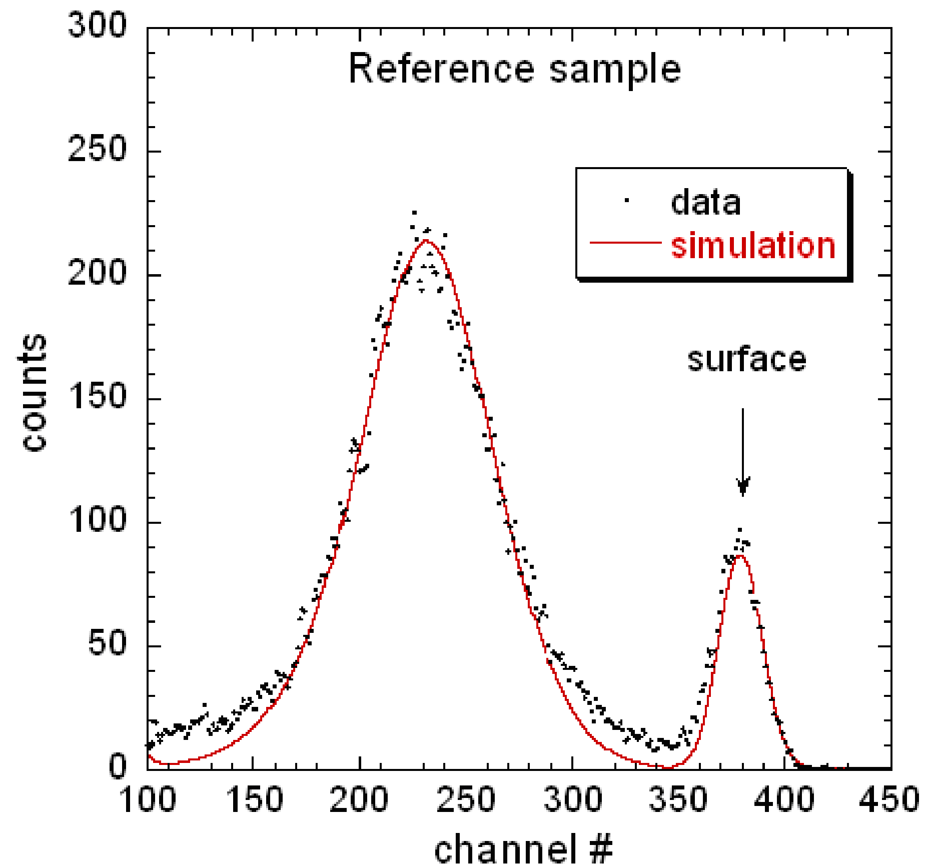

$[Nt]_H$=2.1x10^{17}/cm^2

R_p=280 nm

ΔR=140 nm

HFS: a-Si:H film

RBS

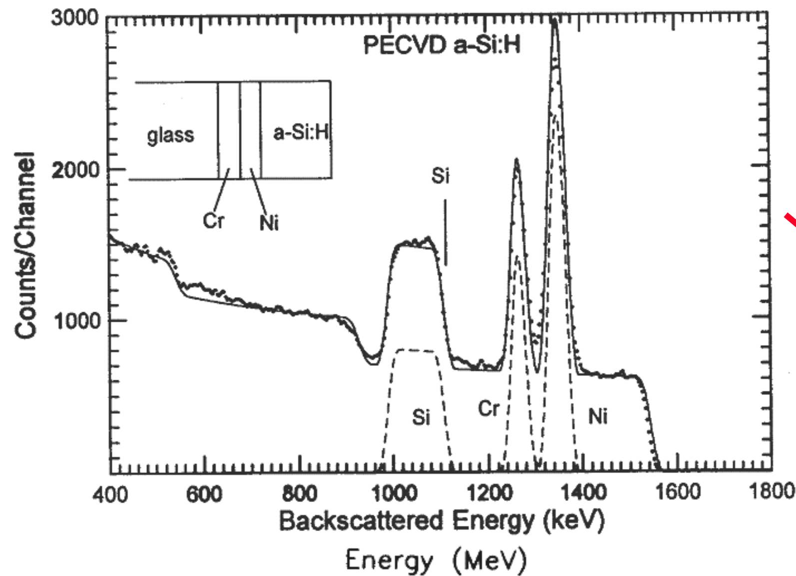

HFS

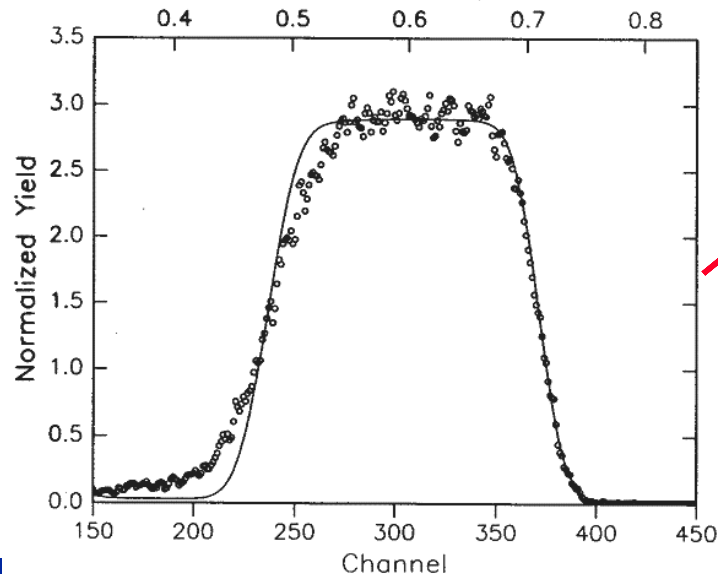

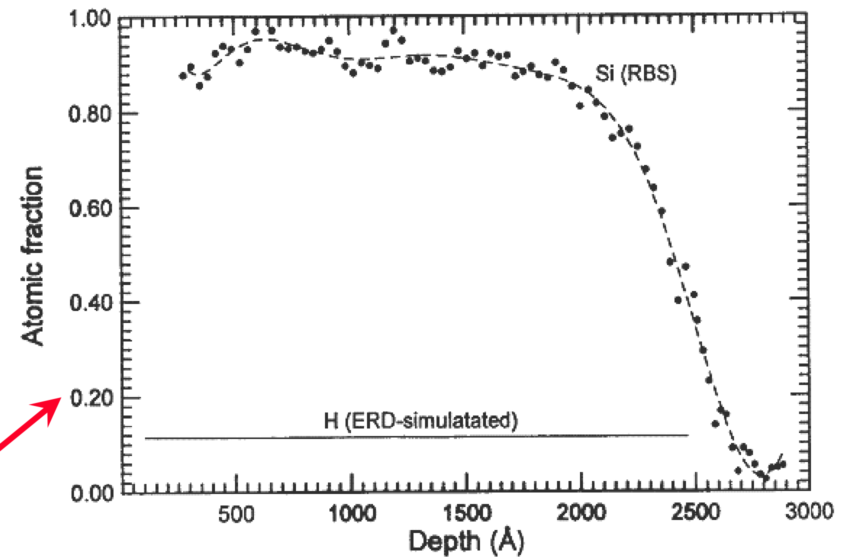

HFS: a-SiN:H film

RBS

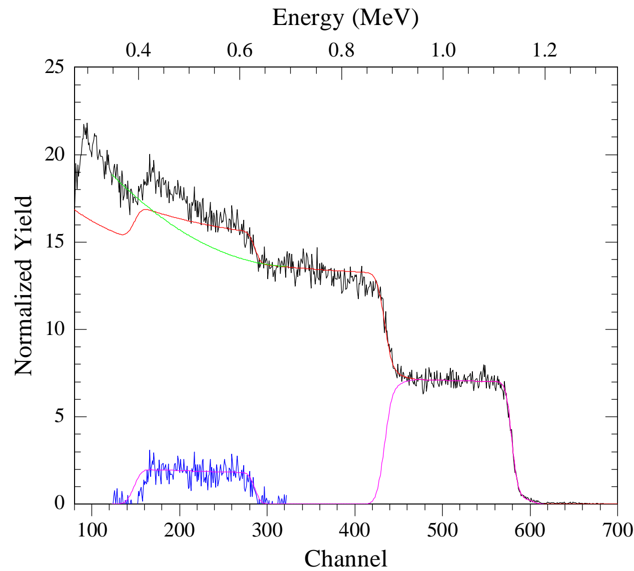

HFS

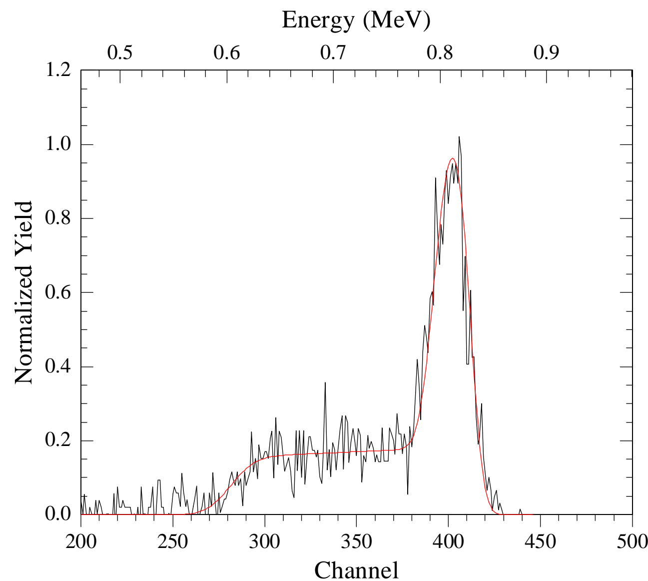

Courtesy: F. Hellman group, 2008

Non-Rutherford Scattering and Nuclear Reaction Analysis

Non-Rutherford Scattering

Non-Rutherford elastic scattering cross sections appear when the ion energy is so high that the ion starts penetrate the Coulomb barrier of the target atom. When the ion penetrates the Coulomb barrier of the target atom, the scattering is from the target atom's nuclear potential and the effect of the nuclear forces for the scattering then become significant.

- For MeV ion beams, this phenomenon can be observed in low Z projectile/target system where the Coulomb barrier is small.
- The cross-section for such nuclear resonance scattering can be many times greater than the Rutherford values.
- Such non-Rutherford scattering has been used to some extent for the detection of light elements (C, N, O, Si) in heavy matrixes

Non-Rutherford Cross-Sections

Summary of Literature on Proton Elastic Scattering Cross Sections Relevant to Low-MeV Proton Backscattering Analysis

Target nucleus	Energy range	Scattering angle	Ref.	Cross section, remarks
^{2}H	2.0—2.8	165 c	51	$\sigma/\sigma_R \approx$ 130—260; data at intervals of 100 keV
^{4}He	1.7—3.0	168 c	51	$\sigma/\sigma_R \approx$ 100-300; data at intervals of 250 keV
^{6}Li	1.2—3.1	164 l	52	$\sigma/\sigma_R \approx$ 1.2 and 15 at 1.2 and 3.0 MeV; a broad peak in the excitation curve (width Γ = 500 keV, $\sigma/\sigma_R \approx$ 30) at E_p = 1.8 MeV
^{7}Li	0.5—1.4	160 c	53	$\sigma/\sigma_R \approx$ 4—8 and 45—70 in the smooth regions of the excitation curve at energies E_p = 1.2—1.8 and 2.4—3.0 MeV; broad peak ($\Gamma \approx$ 200 keV $\sigma/\sigma_R \approx$ 40) at 2.05 MeV; good agreement between data
	0.9—3.7	164 l	51	
	1.3—3.0	167 l	54	
^{9}Be	0.2—1.7	161 c	55	$\sigma/\sigma_R \approx$ 1—2 and 10—11 in the smooth regions below 0.9 and 1.4—2.0 MeV, respectively; the data of Ref. 55 are significantly lower than those of Ref. 56; a broad peak ($\Gamma \approx$ 300 keV $\sigma/\sigma_R \approx$ 40[55] or $\sigma/\sigma_R \approx$ 30[57]; for the peak, see also Ref. 57
	1.6—3.0	146 c	55	
	0.8—2.6	160 c	56	
^{10}B	1.0—3.0	156 c	58	σ/σ_R increases smoothly from 2—7 for energies 1.0—2.0 MeV; a broad peak ($\Gamma \approx$ 200 keV $\sigma/\sigma_R \approx$ 12) at 2.2 MeV; smooth increase of σ/σ_R from 6 (at 2.4 MeV) to 13 (at 3.0 MeV)

Non-Rutherford Cross-Sections (cont.)

Target nucleus	Energy range	Scattering angle	Ref.	Cross section, remarks
^{11}B	0.6—2.0	153 c	59	σ/σ_R decreases from ≈ 2 to 6 in the smooth region above 0.8 MeV
^{12}C	0.7—2.5	170 l	46	σ non-Rutherford at least above 0.3 MeV; σ/σ_R ≈ 2.4—10 and 2.4—15 in the smooth regions at 0.7—1.6 and 1.8—4.3 MeV, respectively; σ/σ_R ≈ 10 at 2.5 MeV; the strong resonance peak (Γ ≈ 40 keV, σ/σ_R ≈ 60) at 1.74 MeV has been used for carbon detection; a low σ/σ_R ≈ 2 minimum at 1.69 MeV
	0.3—4.0	164 l	60	
	0.4—4.3	169 c	61	
^{14}N	1.4—2.3	170 l	46	σ non-Rutherford at least above 0.6 MeV; σ/σ_R ≈ 4—4.5 and 4—9 in the smooth regions at 1.58—1.73 and 1.85—2.3 MeV; strong narrow isolated resonances at 1.74 MeV (Γ ≈ 5 keV, σ/σ_R ≈ 10) and at 3.2 MeV (Γ ≈ 10 keV, σ/σ_R ≈ 50)
	0.9—4.0	161 c	62	
	1.0—4.1	168 c	63	
	0.6—1.8	160 c	64	
	1.9—3.0	166 c	65	
^{16}O	0.8—2.5	170 l	45	σ non-Rutherford above 0.7 MeV, σ/σ_R increases smoothly from 1.0 at 0.7 MeV to 5.7 at 2.5 MeV; another smooth region where σ/σ_R ≈ 6.6—10 between 2.7 and 3.4 MeV; resonances at 2.66 and 3.48 MeV; for angular distributions and the 2.66 MeV resonance, see Ref. 69
	0.8—2.0	172 c	66	
	0.6—4.5	169 l	67	
	0.6—2.0	160 l	68	
	1.4—3.8	168 c	77	Another smooth region where σ/σ_R decreases from ≈ 1.8 to 0.5 at 2.15—2.8 MeV; natural Si target in Ref. 46
	1.0—2.0	150 l	78	
^{19}F	0.8—1.9	165,153 l	42,70	σ/σ_R ≈ 1.4 and 2—1.3 in the smooth regions at 1.0—1.3 and 1.5—1.65 MeV; a resonance at 1.45 MeV
	0.5—1.8	160 c	71	
	0.5—2.1	160 c	72	

Non-Rutherford Cross-Sections (cont.)

Target nucleus	Energy range	Scattering angle	Ref.	Cross section, remarks
^{23}Na	0.6—1.5 0.5—1.0	158 c 160 l	73 56	$\sigma/\sigma_R \approx$ 0.9—1.1 in the smooth region at 1.0—1.4 MeV;[73] the data from Ref. 56 are significantly lower than those of Ref. 73
^{24}Mg	0.7—2.5 0.4—3.9	170 l 164 l	47 74	σ non-Rutherford above 0.8 MeV; $\sigma/\sigma_R \approx$ 1.05—1.1 and 1.3—1.5 in the smooth regions at 0.85—1.4 and 1.66—1.85 MeV; resonances at 0.83, 1.48, 1.62, and above 1.9 MeV; natural Mg used as target in Ref. 47
^{27}Al	1.0—2.4 1.4—2.3	170 l 164 l	48 75	σ non-Rutherford at least above 1.0 MeV; many sharp overlapping resonances, no smooth regions wider than 50 keV above 1.2 MeV; σ/σ_R < 3 up to 2.4 MeV; yield curve without absolute cross section scale in Ref. 75
^{28}Si	1.5—2.2 2.0—5.0	170 l 165 c	46 76	σ non-Rutherford at least above 1.5 MeV; σ/σ_R decreases smoothly from $\approx$2.2 to 1 for energies from 1.7 to 2.05 MeV ($\Gamma \approx$15 keV), isolated resonance at E_{He} = 4.79 MeV; see also Refs. 118 to 120
^{31}P	1.0—2.0	165 l	79	σ non-Rutherford at least above 1.0 MeV; $\sigma/\sigma_R \approx$ 1.05 and 1.2 in the smooth regions at 1.0—1.2 and 1.3—1.45 MeV. Resonances at 1.25, 1.52, 1.59, 1.72—1.74, and 1.90 MeV

Non-Rutherford cross sections

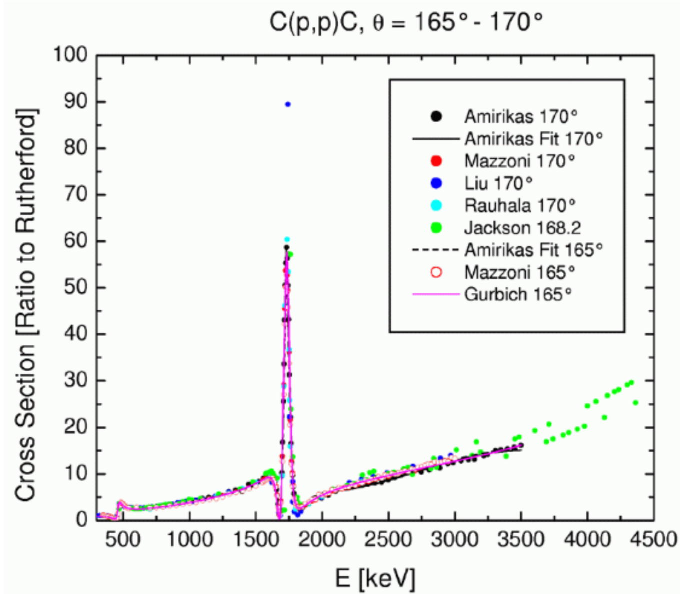

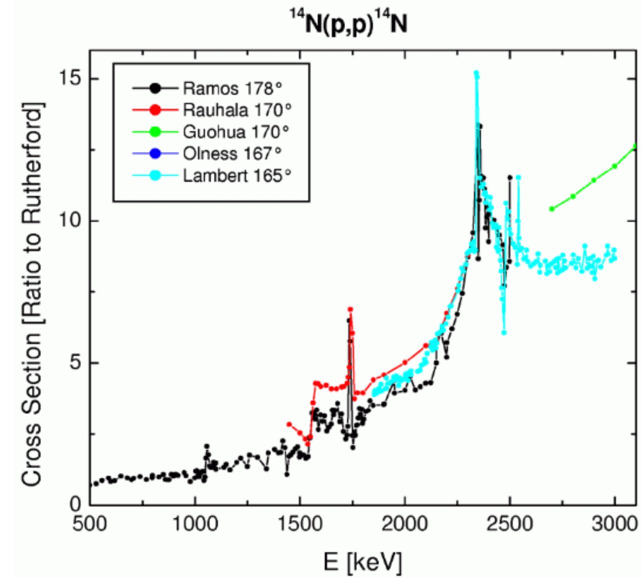

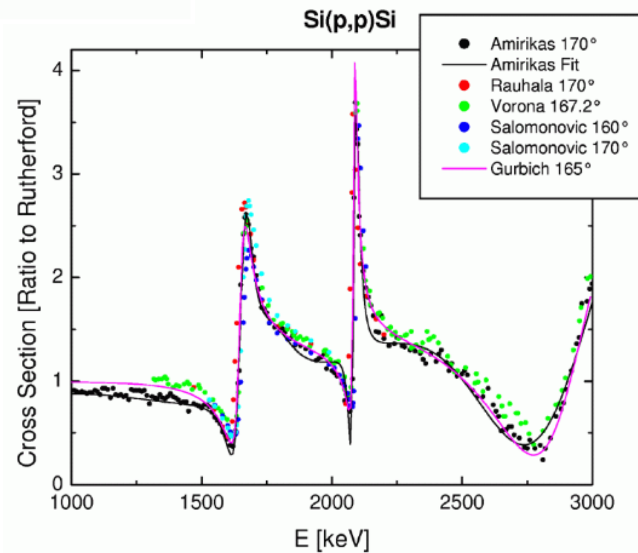

Non-Rutherford scattering: Example 1: SiO_2

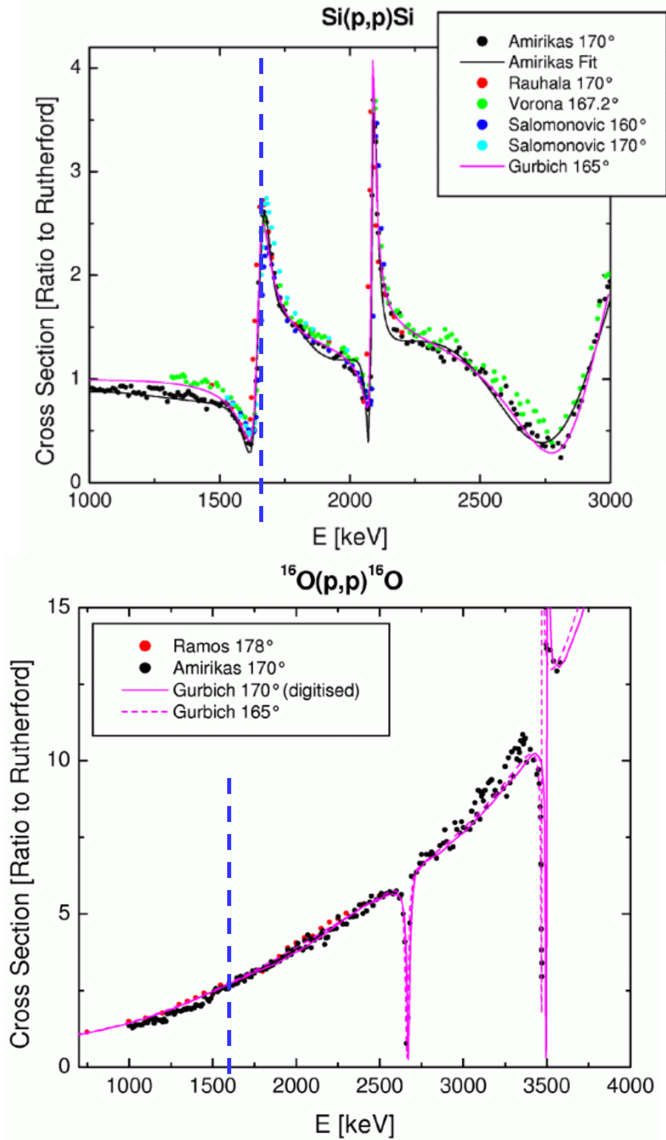

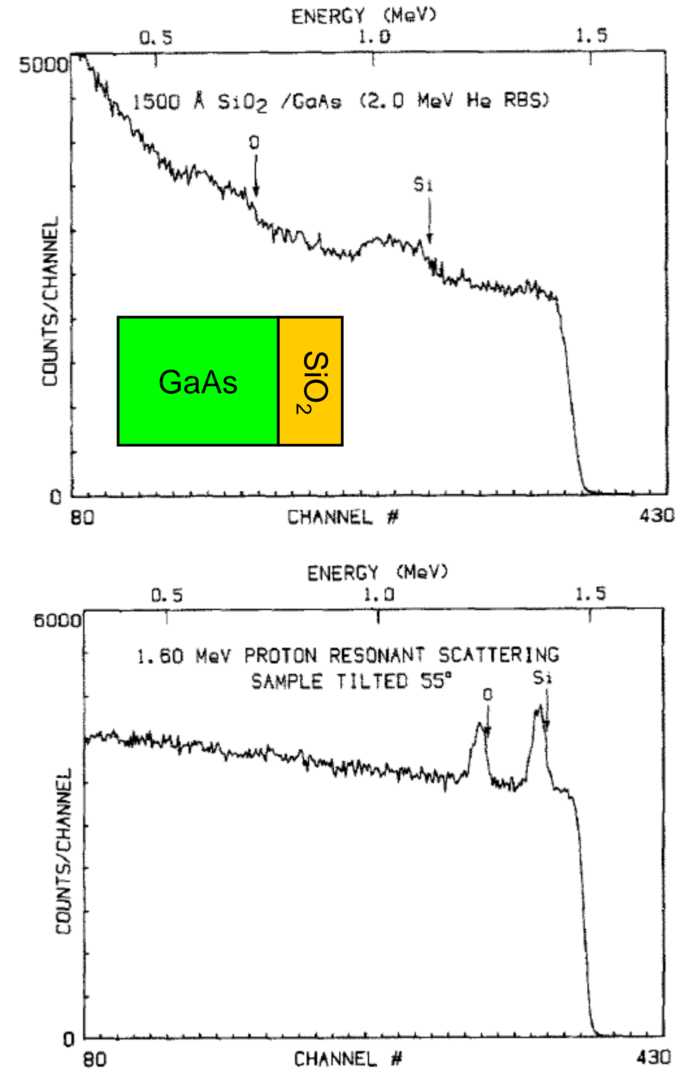

Fig. 4. Backscattering spectra of 2.0 MeV He-RBS (a) and 1.60 MeV PRS (b) of a 1500 Å SiO_2 film on GaAS.

K. M. Yu et al., Nucl. Instrum. Meth. **B30** (1988) 551-556

Non-Rutherford scattering: Example 1: SiC

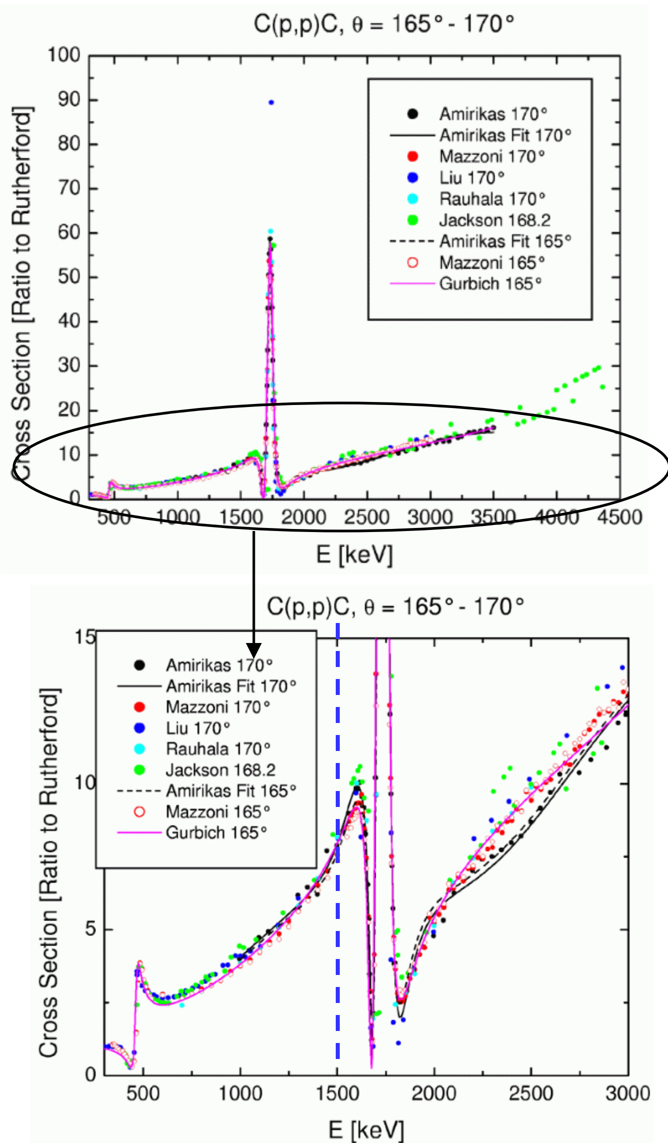

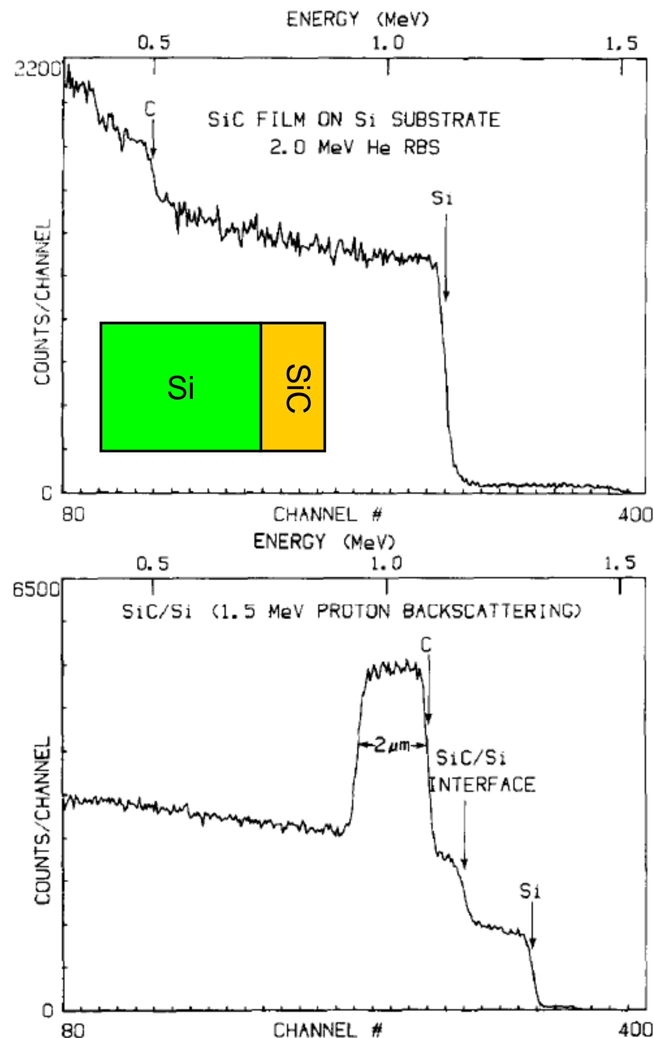

Fig. 5. Backscattering spectra with 2.0 MeV He particles (a) and 1.50 MeV protons (b) from a sample of 2μm SiC film on Si substrate.

K. M. Yu et al., Nucl. Instrum. Meth. **B30** (1988) 551-556

Nuclear Reaction Analysis (NRA)

^{14}N (d,p) ^{15}N

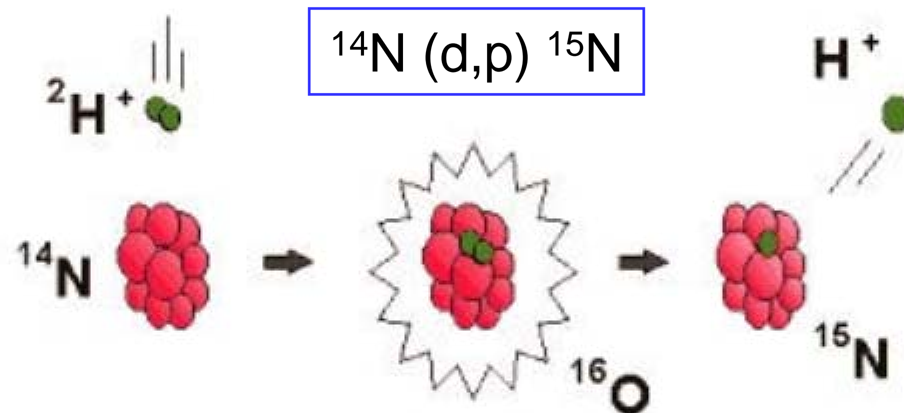

- **When the incident beam energy exceeds a certain threshold value, other energetic particles appear in the spectrum.**
- **The detection of these particles usually provide information which is not obtainable from RBS.**
- **The NRA technique is very useful as a tool for <u>the detection and profiling of light elements</u> in heavy matrix.**
- **In many cases such particle-particle NRA can be carried out in a RBS setup with only minor modifications.**

Some useful particle-particle reactions

Nucleus	Reaction	Incident Energy (MeV)	Emitted Energy (MeV)	Approx. cross section (mb/sr)
^{2}H	^{2}H (d,p) ^{3}H	1.0	2.3	5.2
^{2}H	^{2}H (3He,p) ^{4}He	0.7	13.0	61
^{6}Li	^{6}Li (d,α) ^{4}He	0.7	9.7	35
^{7}Li	^{7}Li (p,α) ^{4}He	1.5	7.7	9
^{11}B	^{11}B (p,α) ^{8}Be	0.65	5.57 (αo)	0.7
		0.65	3.70 (α1)	550
^{12}C	^{12}C (d,p) ^{13}C	1.2	3.1	35
^{15}N	^{15}N (p,α) ^{12}C	0.8	3.9	15
^{18}O	^{18}O (p,α) ^{15}N	0.73	3.4	15
^{19}F	^{19}F (p,α) ^{16}O	1.25	6.9	0.5
^{23}Na	^{23}Na (p,α) ^{20}Ne	0.592	2.238	4
^{31}P	^{31}P (p,α) ^{28}Si	1.514	2.734	16

NRA Example: GaNAs dilute nitride

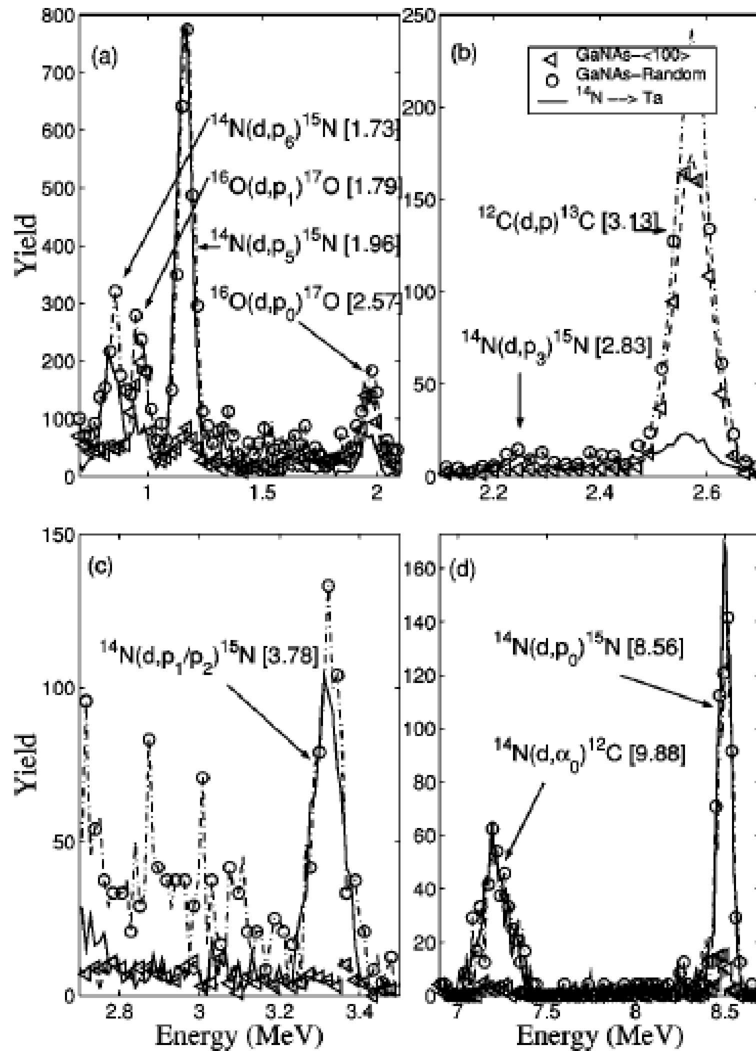

1.3 MeV deuterium ions

$^{14}N(d,p)^{15}N$ and $^{14}N(d,\alpha)^{12}C$ reactions

GaNAs film with ~4% N

FIG. 1. Experimental NRA yields from GaNAs (⟨100⟩ and random direction) and ^{14}N implanted Ta. Triangles and rings denote ⟨100⟩ and random yields, respectively. The values in the square brackets are the initial particle energies in mega-electron-volts before the mylar foil in front of the detector. Figures (a), (b), (c), and (d) corresponds to the reaction yield in different regions of particle energy.

T. Ahlgrena et al., Appl. Phys. Lett. **80**, 2314 (2002).

Ion Channeling

Ion channeling

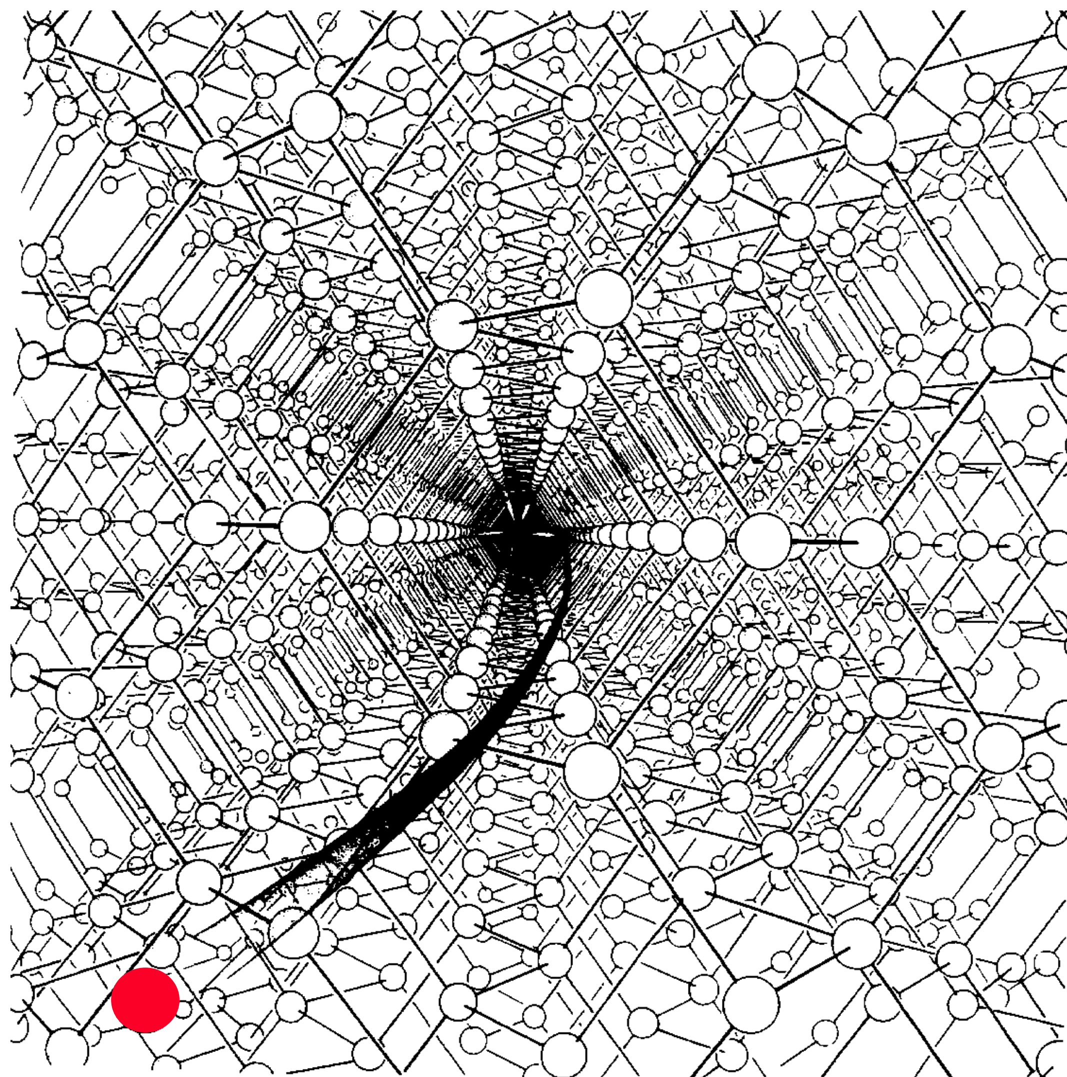

Ion Channeling

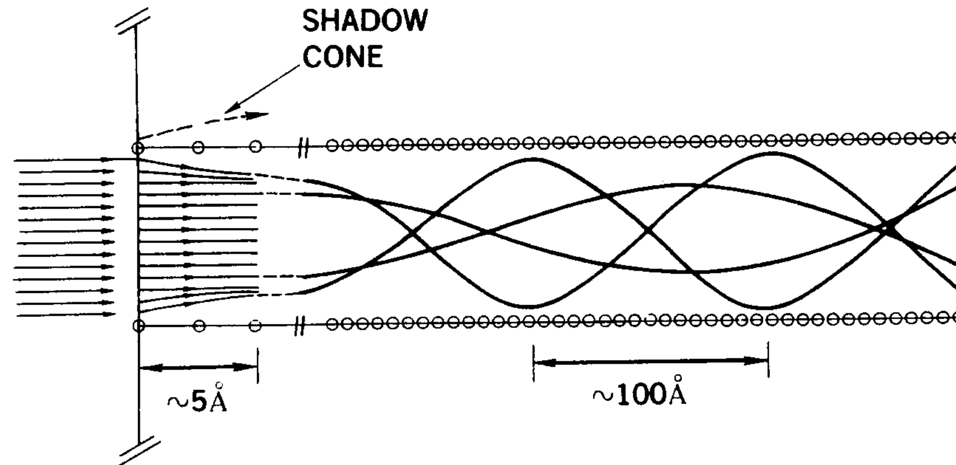

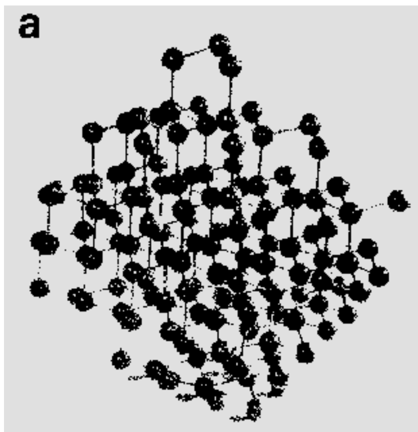

random

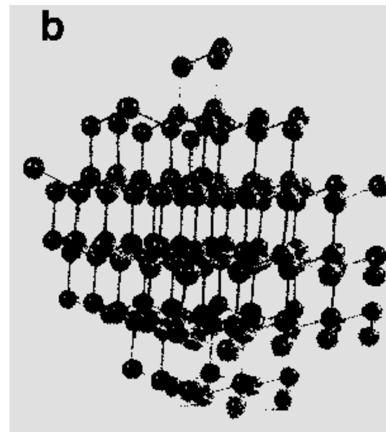

Planar channel

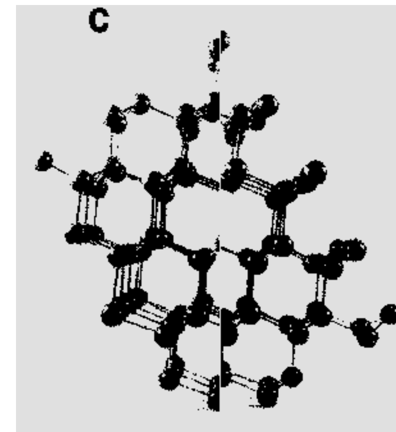

Axial channel

Ion Channeling

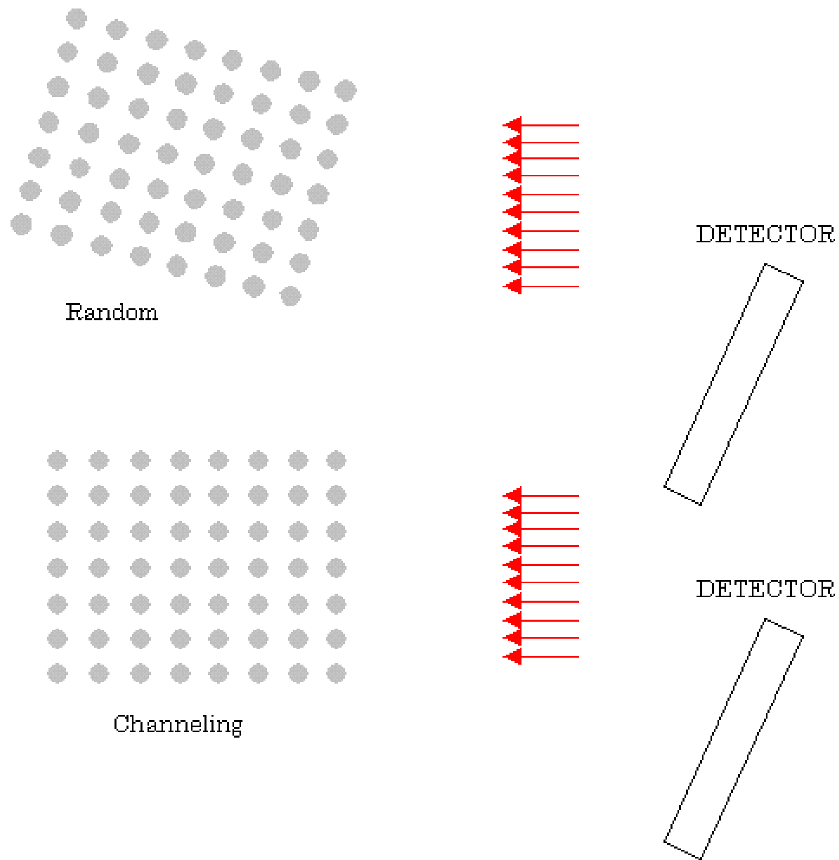

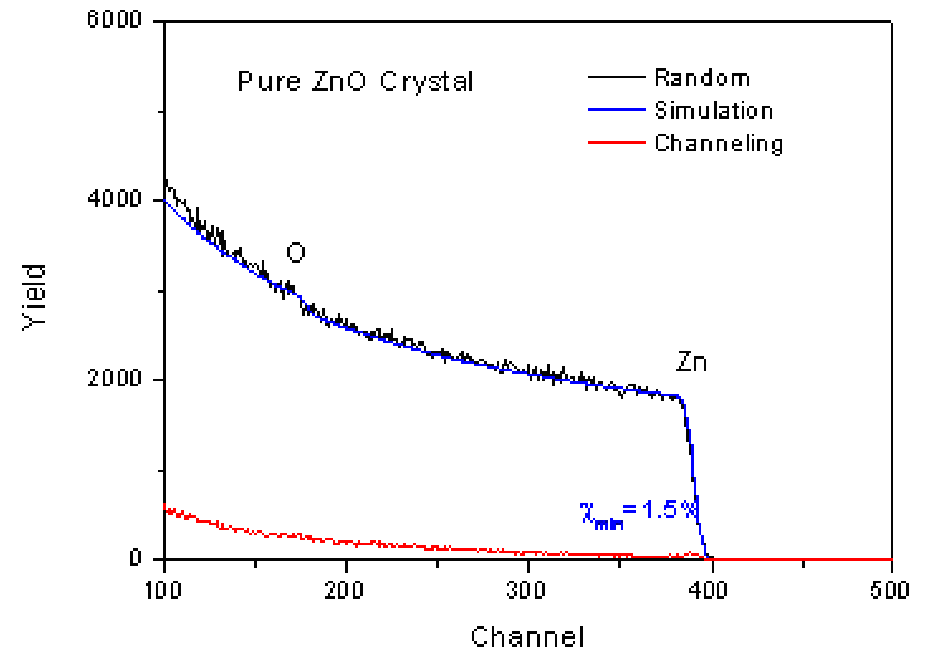

Kobelco Steel Group

Ion Channeling:
minimum yield and critical angle

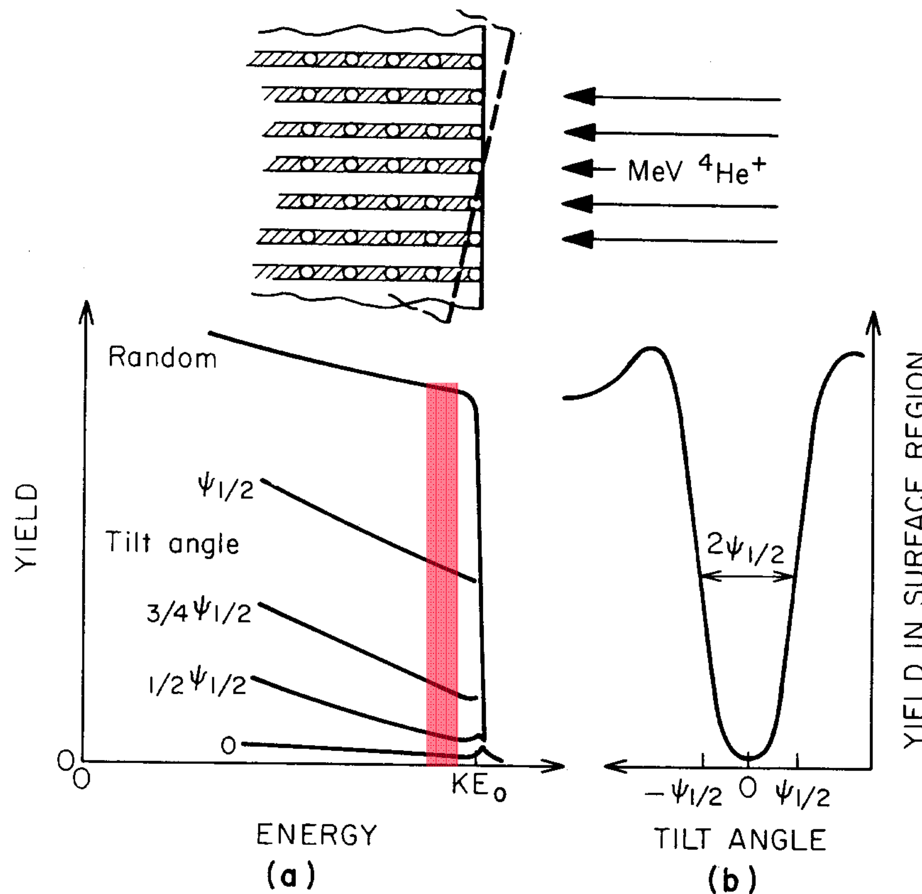

Two important parameters to characterize channeling results:

1. Minimum yield:

$$\chi_{\min} = \frac{Y_{channeled}}{Y_{random}}$$

~0.02-0.06

2. Critical half-angle, $\psi_{1/2}$

   indicates presence of defects responsible for beam dechanneling

Ion Channeling:
minimum yield and critical angle

Minimum Yield, χ_{min}

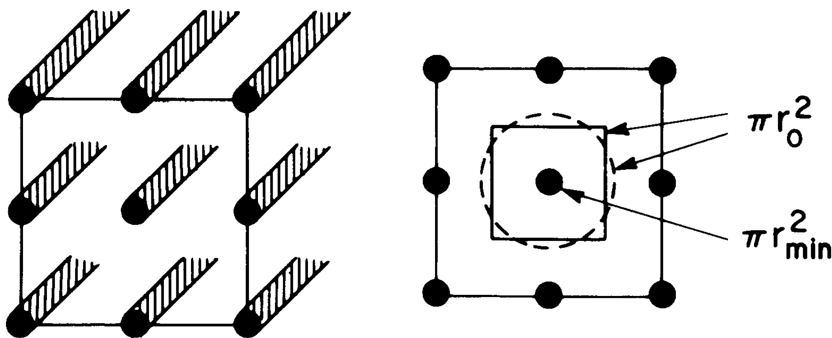

$$\chi_{\min} = \frac{Y_{channeled}}{Y_{random}}$$

$$\chi_{\min} \approx \frac{\pi r_{\min}^2}{\pi r_o^2} \sim 0.02 - 0.05$$

Critical half-angle, $\psi_{1/2}$

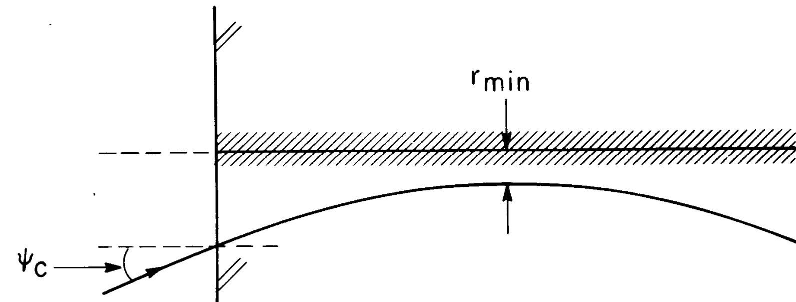

$$\Psi c = \frac{1}{\sqrt{2}} \left(\frac{2Z_1Z_2e^2}{Ed}\right)^{1/2} \left\{ \ln\left[\left(\frac{Ca}{\rho}\right)^2 + 1\right] \right\}^{1/2}$$

where d is the distance of atoms in a row, a is the Thomas-Fermi screeing distance, r is rms thermal vibration

$$\Psi_{1/2} \sim \Psi_c \sim \left(\frac{2Z_1Z_2}{E}\right)^2 \sim 0.5 - 1^o$$

Dechanneling by defects

Dechanneled

Channeled

Backscattered

MeV
$^{4}He^{+}$

Small angle dechanneling-
line defects

Perfect crystal
channeling

Direct scattering-
point defects

Homo- and Heteroepitaxy

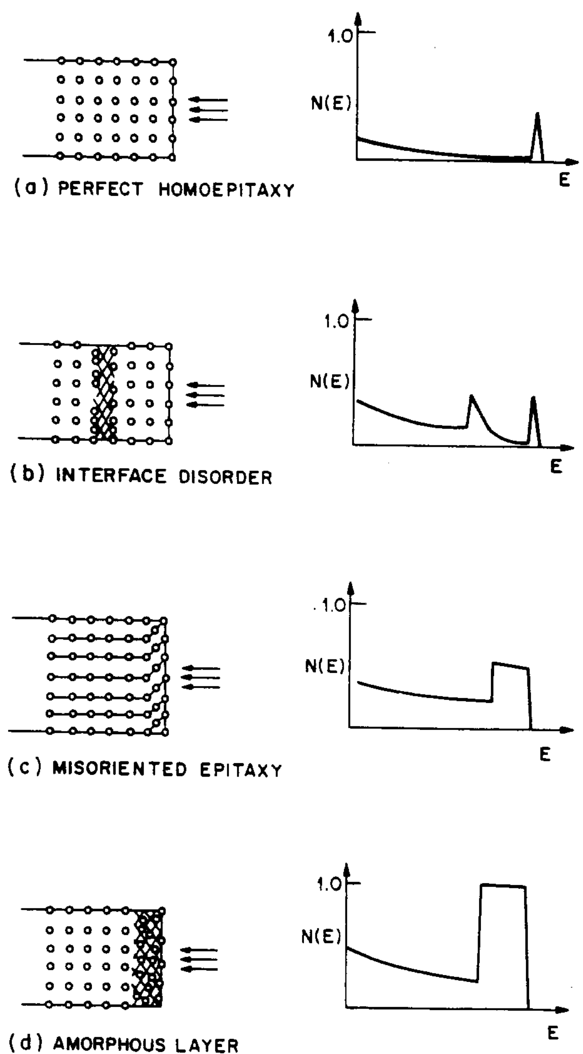

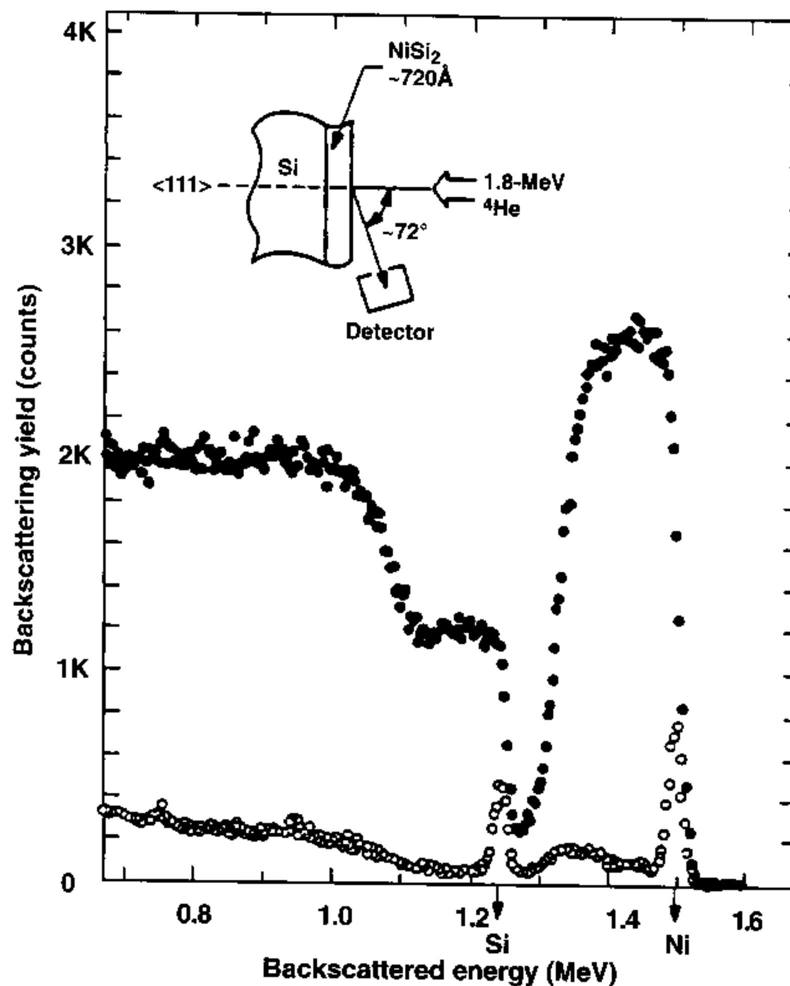

FIG. 10.24. Random and <111> channeling spectra for a 72 nm $NiSi_2$ epitaxial film on a (111) Si substrate (from Chiu *et al.*, 1980).

Channeling: Heteroepitaxy

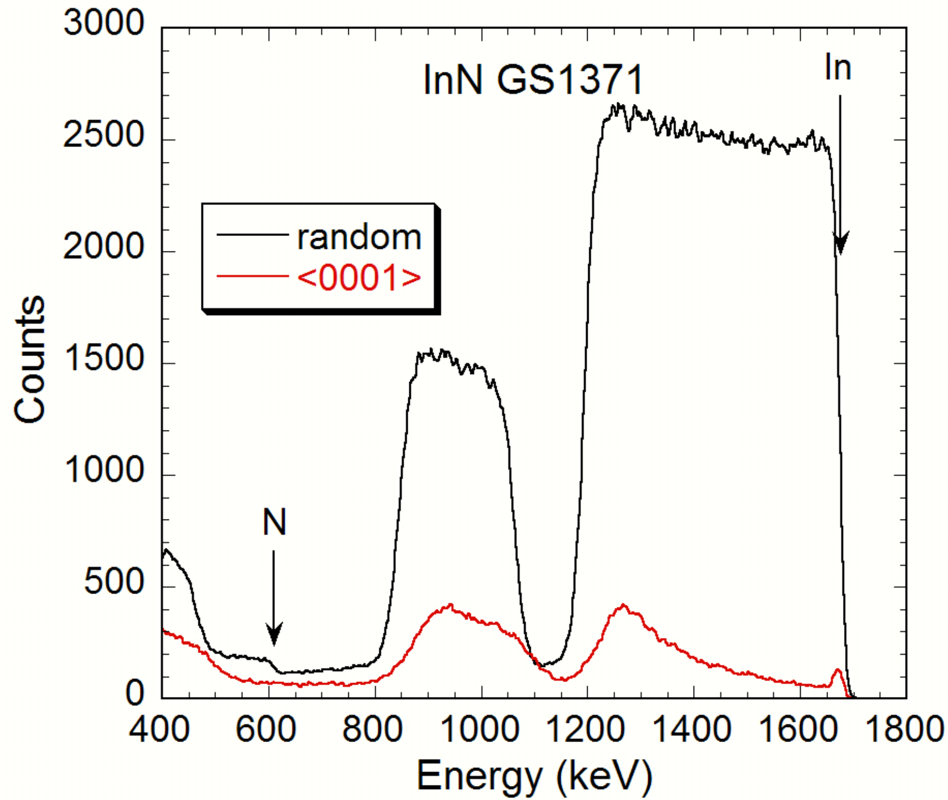

~530nm InN on 210 nm GaN

K. M. Yu et al., LBNL 2004.

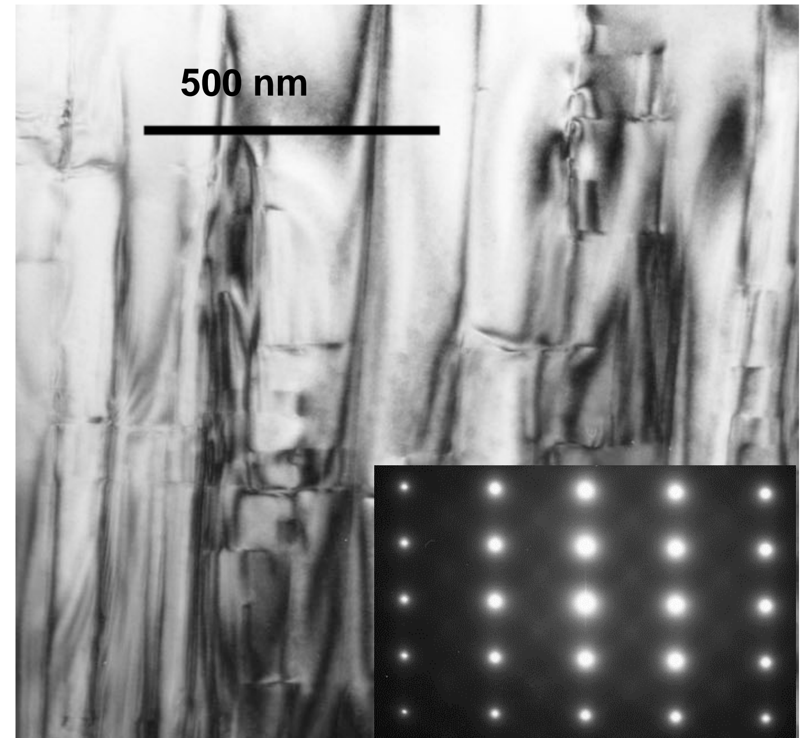

Z. Liliental-Weber

Amorphous layer analysis

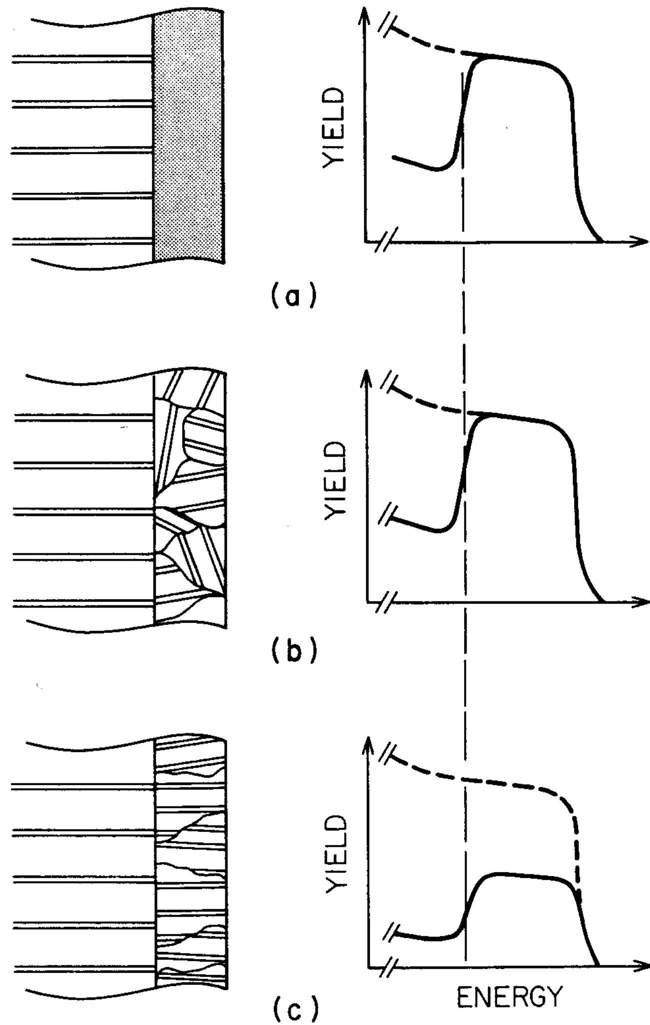

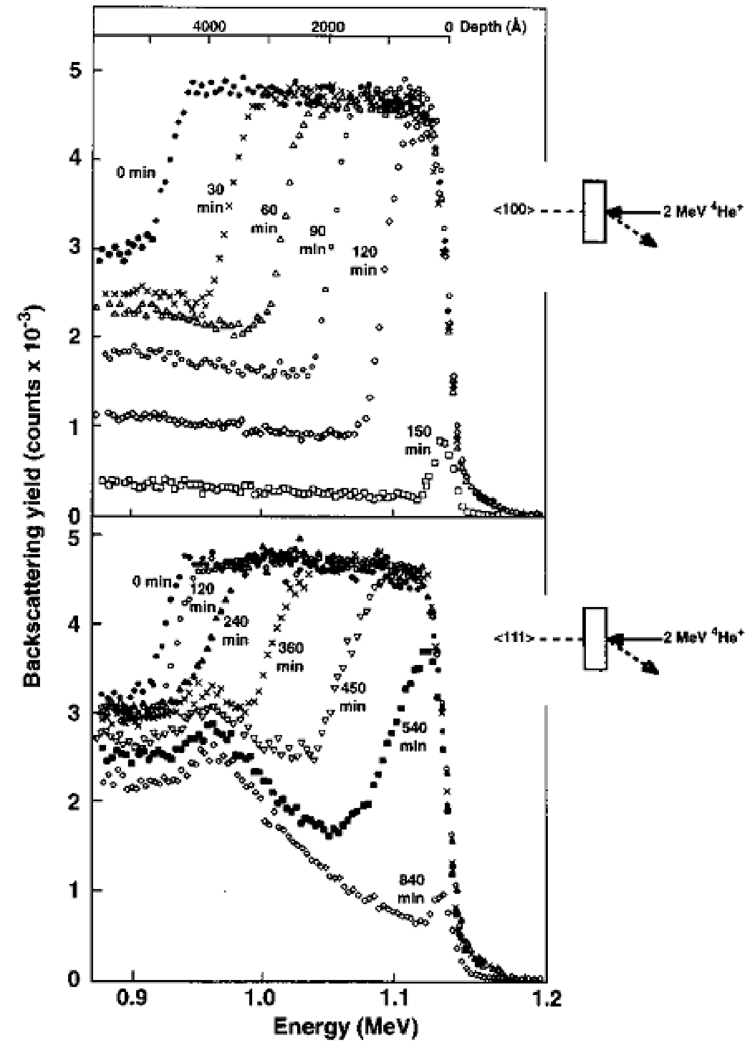

Channeling: Impurity Lattice Location

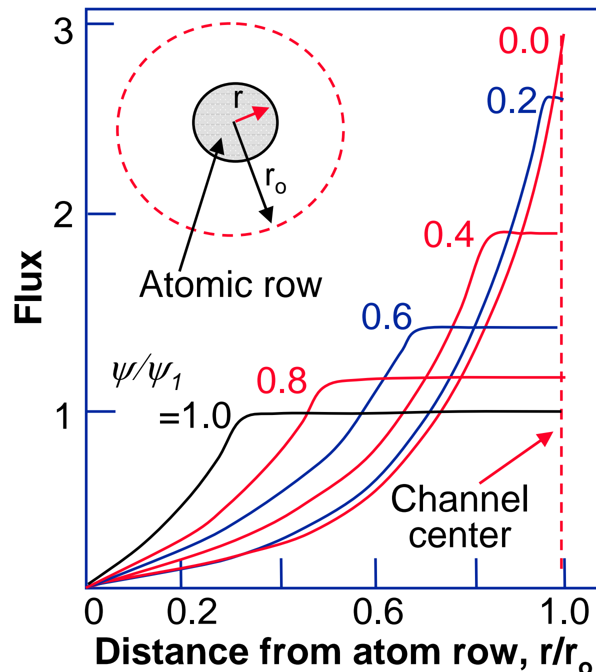

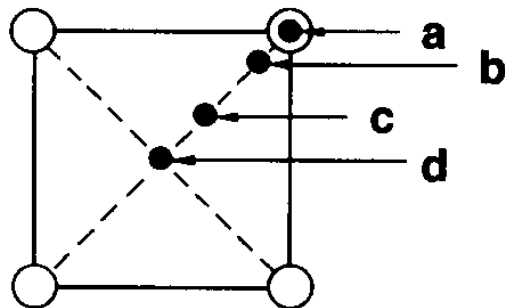

Channel cross section

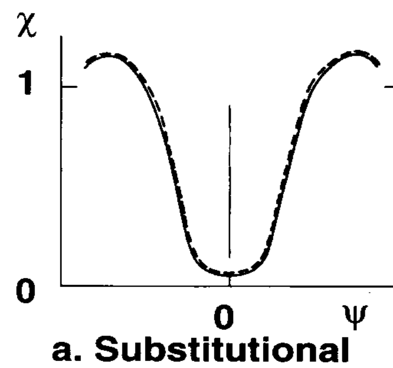

a. Substitutional

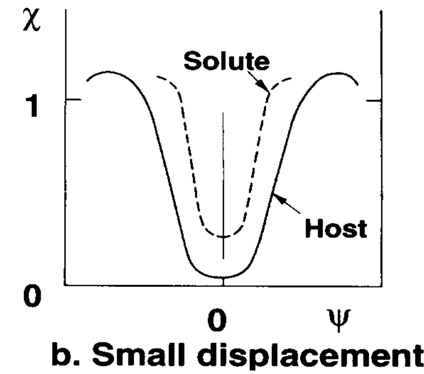

b. Small displacement

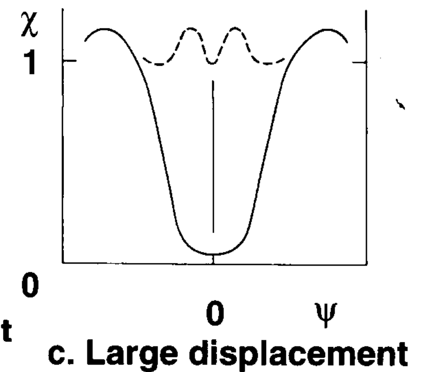

c. Large displacement

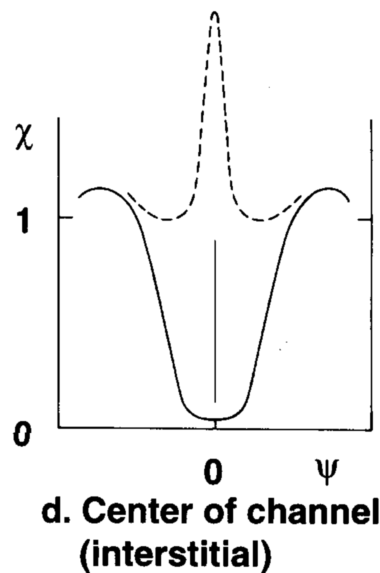

d. Center of channel (interstitial)

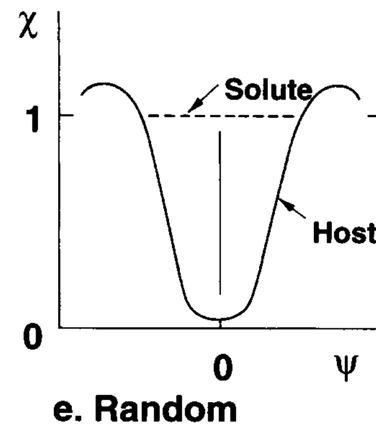

e. Random

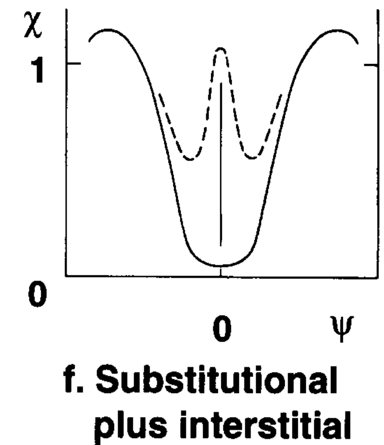

f. Substitutional plus interstitial

Experimental techniques :
combined channeling RBS/PIXE

Rutherford backscattering (RBS)

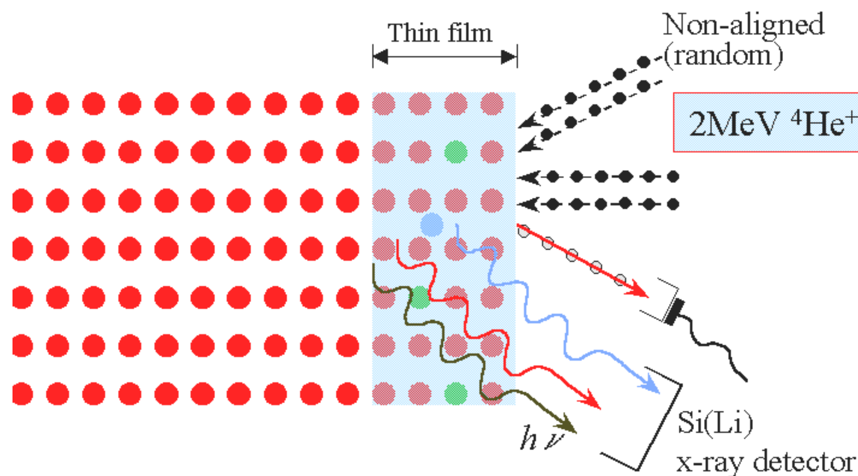

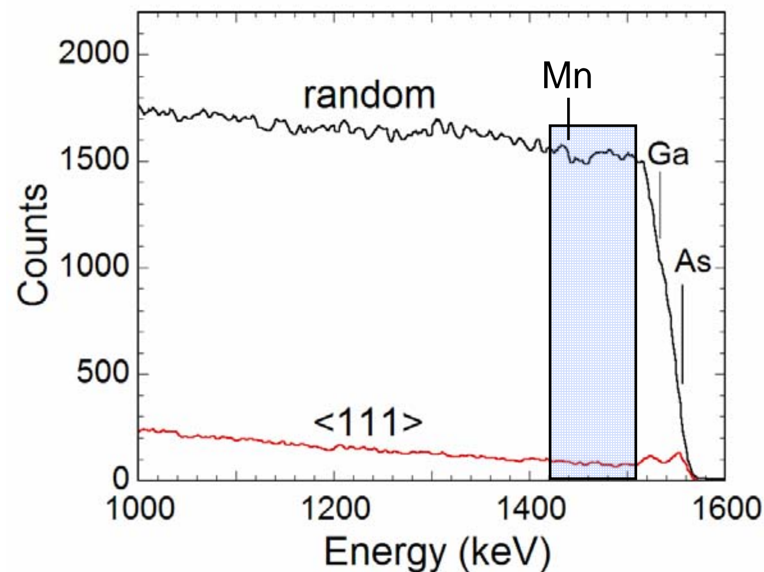

Particle-induced x-ray emission (PIXE)

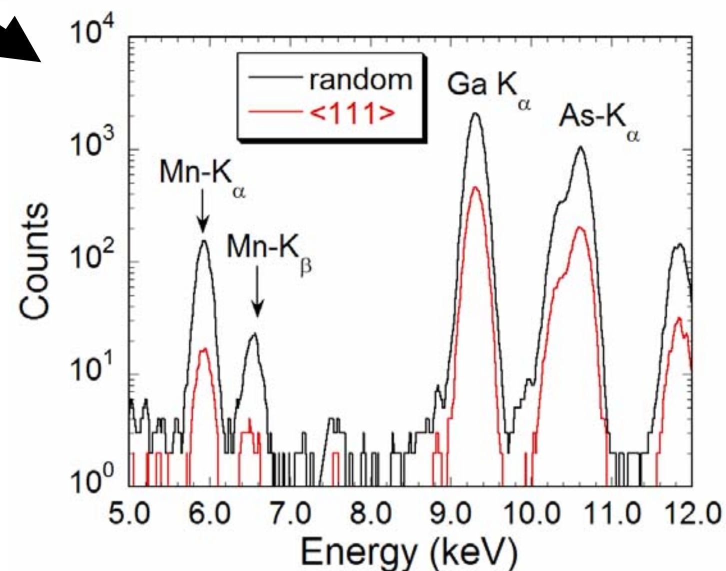

c-RBS: crystalline quality of film (from GaAs backscattering yields)

c-PIXE: substitutionality of Mn atoms w.r.t. host GaAs

Channeling: $Ga_{1-x-y}Be_yMn_xAs$

Channeling RBS/PIXE:

- presence of interstitial Mn in GaAs
- $[Mn_I]$ increases with Be doping
- Mn_I reduces T_C

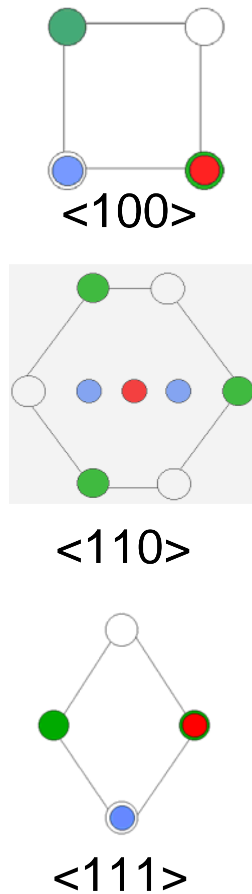

Cation
Anion
Tetrahedral interstitials
Hexagonal interstitials

K. M. Yu et al. 2003.

Examples of applications for IBA

- Thin film analysis: composition and thickness
- Multilayer analysis: identification of reaction products; obtaining reaction kinetics, activation energy, and moving species
- Composition analysis of bulk garnets
- Depth distribution of heavy ion implantation and/or diffusion in a light substrate
- Surface damage and contamination
- Providing calibration samples for other instrumentation such as secondary ion mass spectroscopy and Auger electron spectroscopy
- Defect depth distribution due to ion implantation damage or residue damage from improper annealing
- Lattice location of impurities in single crystal
- Surface atom relaxation of single crystal
- Lattice strain measurement of heteroepitaxy layers or superlattices